INTERNATIONAL JOURNAL OF HYDROGEN ENERGY 44 (2019) 28007–28030

Available online at www.sciencedirect.com

ScienceDirect

journal homepage: www.elsevier.com/locate/he

Review Article

Effect of hydrogen in advanced high strength steel materials

Sandeep Kumar Dwivedi[*], *Manish Vishwakarma*

Department of Mechanical Engineering, Maulana Azad National Institute of Technology, Bhopal, 462003, Madhya Pradesh, India

HIGHLIGHTS

- AHSS materials are susceptible towards the hydrogen embrittlement.
- Ductility of AHSS materials are reduced significantly with and without reduction in ultimate tensile strength.
- Behavior of TWIP steels in hydrogen environment was inconsistent.
- Traps can reduce the hydrogen susceptibility in AHSS material.
- Coatings are used to reduce hydrogen penetration.

ARTICLE INFO

Article history:
Received 16 April 2019
Received in revised form
10 August 2019
Accepted 18 August 2019
Available online 11 September 2019

Keywords:
Advance high strength steel
Hydrogen embrittlement
Fractograpy examination
LIST
SEM

ABSTRACT

The effect of hydrogen in AHSS material (automobile and structural component) was discussed. Dual Phase steels were highly susceptible to hydrogen-related failure when working on hydrogen environment. The influence of hydrogen on TRIP steel was seen during fractographic examination where the brittle transgranular fracture was presented. TWIP steels results were inconsistent. The mechanisms which were responsible for crack growth are discussed. LIST and SSRT testing were performed for mechanical properties evaluation and SEM and TEM were used for microstructural examination of fractured samples. Simultaneous preventing methods to reduce hydrogen embrittlement such as coating, alloying and providing diffusion layer were discussed.

Contents

* *Corresponding author.*
E-mail address: Sandeep0183@gmail.com (S.K. Dwivedi).

https://doi.org/10.1016/j.ijhydene.2019.08.149

Introduction

High strength steel materials (HSS) are used in many industrial applications such as in automotive, automobile components and transportation due to their high strength to weight ratio and excellent mechanical properties (strength and elongation) better than the conventional steels. As the applicability of high strength materials was increased, modification on existing high strength steel materials had done and a new Advanced High Strength Steel Materials (AHSS) are arrive and applicable in the existing areas where high strength materials were used because of their superior quality (strength). These AHSS materials are having good formability when compared to existing steels. Some AHSS materials are Dual-phase (DP) steel, Transformation induced plasticity (TRIP), Twinning-induced plasticity (TWIP) steels and Quenching and partitioning (Q&P) steels. They are categorized on the basis of their strength and elongation properties. In the last few decades, considerable developments in AHSS have been done and they are accepted for auto construction. Fig. 1 shows the comparison of mechanical properties (strength and ductility) between conventional and AHSS. The microstructure of conventional steel and AHSS are totally different from each other. Conventional steels are having ferrite microstructure whereas AHSS are having microstructure comprises of different phases such as ferrite, bainite, austenite, and martensite [1,26].

Hydrogen is introduced in steel during the steel making process and working environment condition like (corrosive environment). This absorbed hydrogen is one of the main causes for reduced mechanical properties of steels and sub-critical crack growth, resulting in the arrival of catastrophic failure during service condition without giving any significant signature below its permissible limit of stress [7,8]. This effect of absorbed hydrogen causing failure of high strength materials well below its permissible value with considerable changes in ductility is called hydrogen embrittlement [HE] which occurs when a critical level of hydrogen is reached in steel [1–6]. Due to the effect of hydrogen, the ductility of material is decreased with little or no effect on yield strength

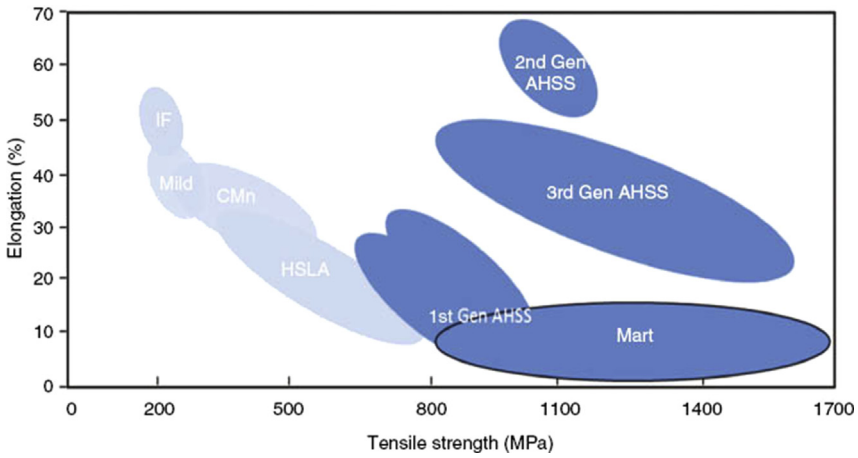

Fig. 1 – Comparison of strength and ductility of AHSS and traditional steels used for automobile components construction, where IF: interstitial free steel, BH: bake hardenable steel, CMn: carbon manganese steel, HSLA: high strength low alloy steel [26,41].

as well as tensile strength. Hydrogen produced as a result of corrosion reaction may be diffused in steel auto components and causing hydrogen delayed failure or fracture [9]. HE may be classified into two categories i.e. internal hydrogen embrittlement (IHE) and external or environmental hydrogen embrittlement (EHE). In the case of IHE, hydrogen atom is actually inside the base material or available in solute metal. Hydrogen may get diffused inside the material during steel making or fabrication process. Whereas in EHE case, hydrogen atom gets diffused from the surface of a base material by adsorption followed by absorption process such as during high-pressure hydrogen storage tank (hydrogen bearing environment). During both cases, the critical stress and hydrogen concentration are required for the material to be susceptible to HE [36,37]. From some studies it was found that the car machinery is subjected to a very high impact load or stress at the time of the accident so, to resist this high impact stress, a sufficient amount of toughness must be provided in automotive steels and subcomponents of car body so that they will not fracture directly. There are many factors which are responsible for reducing the toughness of particular steel components such as hydrogen during the service condition. So, these factors are required to be understood and must be taken care of by car manufacturer [3,9].

The chief aim of the automotive industry is to achieve the maximum strength and stiffness of the particular material used for manufacturing the subcomponents of a car with weight reduction and low cost. Sometimes the weight reduction is the prime motive with the same value of strength and stiffness. Aluminium is light metal but its stiffness value is less and cost is high when compared to steel. To achieve the above requirement, AHSS materials are used because they have a good combination of strength and weight and also very much suitable for the automotive industry. But one drawback of using AHSS is that they are affected or susceptible to hydrogen embrittlement failure [10,11]. Steel whose strength is more than 1000 MPa is more prone towards the HE [188]. This HE degrades the mechanical properties (strength, toughness, and ductility) of material, causing sub-critical crack growth, fracture initiation and a brittle failure (Intergranular or Transgranular). So, for an appropriate understanding of hydrogen-related failure, in the future, detailed research will be carried out to know how hydrogen atoms can interact with the AHSS. Wide variety of mechanisms available to explain the effect of hydrogen in AHSS materials are hydrogen enhanced decohesion mechanism (HEDE), adsorption induced dislocation emission (AIDE), hydrogen enhanced localized plasticity (HELP), hydrogen enhanced macroscopic plasticity (HEMP), hydrogen changed micro-fracture mode (HAM), decohesive hydrogen fracture (DHF), Hydrogen assisted microvoid coalescence (HDMC) and mixed modes fracture (MF) [3,8,13,15,20,21,24,26,138–150]. Sometimes a single mechanism is responsible for hydrogen-related failures such as HE and sometimes a combination of several mechanisms as mentioned above are responsible for degradation in mechanical properties and final brittle fracture due to the effect of hydrogen. As a result of the simultaneous action of these mechanisms in the hydrogen environment, subcritical crack growth is taking place in the material. For the complete understanding and meaning full knowledge of sub-critical crack initiation, propagation and mechanism cause failure of material, macro and micro-scale fractography examination are urgently required [2,12–24]. Methods by which hydrogen atom gets diffused in the metal lattice are electroplating, cathodic charging, and welding process. It was also found from the literature that current density plays an important role during cathodic charging for the absorption of hydrogen in AHSS materials. If the current density is high then chances of hydrogen atoms to get diffused in a metal lattice are increased [34,35].

Presence of carbides also responsible for hydrogen-related failure. By tempering treatment, carbide size varies, mobile hydrogen traps between the carbide matrix interfaces and increases the resistance towards mechanical properties degradation due to lower hydrogen [185]. It was also found that both size and type of carbide formation play an important role in trapping capacity of hydrogen and efficiency of tungsten (W)-based precipitates [186]. Hydrogen trapping ability of

TiC and its effect in HE characteristics of Fe–C–Ti alloys was investigated by Depover and Verbeken. They found that after quenched and tempered condition, hydrogen-related degradation phenomena (ductility loss) reduced due to more hydrogen trapping capacity of TiC. As the number of trapping sites is increasing, the hydrogen diffusion coefficient of alloy reduces [187].

There are several AHSS available and they have different properties from each other are shown in Table 1. Some AHSS materials are having high mechanical properties and different microstructure. Dual-phase (DP) steel is generally considered as a first-generation AHSS. They have a ferritic matrix with the dispersion of the martensite islands. Transformation induced plasticity (TRIP) steel are having several microstructures such as ferrite matrix with austenite, bainite, and martensite. Twinning-induced plasticity (TWIP) steels are having entirely austenite microstructure due to the availability of manganese [1,10,23]. Quenching and partitioning (Q&P) steels have a new class of AHSS material. They are having mechanical properties greater than all other AHSS materials. These steels are used in many areas such as car industries, shipbuilding, aircraft and civil construction [1,25–27].

There is a wide variety of testing technique are available for knowing the consequence of hydrogen in mechanical properties of AHSS materials such as linearly increasing stress test (LIST) and slow strain rate test (SSRT) [29,30,188,189]. Microstructure examination has been done by Scanning electron microscopy (SEM), field emission scanning electron microscopy (FESEM) and transmission electron microscopy (TEM) [2,26,33]. By microstructure examination, effect and consequences of hydrogen in AHSS materials (internal microstructure) are known. Diffusible hydrogen contents in AHSS material are determined by various techniques such as glycerin method, vacuum hot-extraction method, mercury method and gas chromatography technique [28]. A most suitable technique to measure the diffusible hydrogen contents when hydrogen is available in very low quantity is mercury method. Temperature-programmed desorption (TPD) is also very important techniques to measure the diffusible hydrogen content in AHSS materials. This technique was also used for the study of hydrogen movement in the lattice and hydrogen-related failure [31,32]. Permeation experiment was performed to determine the effect of diffusible hydrogen in deformation change of different steel. It was found that HE susceptibility highly depends on the microstructure and strength level [190]. Hydrogen embrittlement is a very well-known phenomenon for conventional as well as AHSS materials. As the strength of the material is increasing, chances of hydrogen-related failure may get increased if machine or specimen is working on hydrogen environment.

Table 1 – Mechanical properties of various AHSS [154].

SN	Steel Grade	YS (MPa)	UTS (MPa)	Total Elongation (%)
1	HSLA 350/450	350	450	23–27
2	DP 300/500	300	500	30–34
3	DP 350/600	350	600	24–30
4	DP 500/800	500	800	14–20
5	DP700/1000	700	1000	12–17
7	CP 700/800	700	800	10–15
8	TRIP 450/800	450	800	26–32
9	MS 1250/1520	1250	1520	4–6

Hydrogen is recognized as a future fuel as it has high electrical energy. The literature said that during the little amount of hydrogen combustion, a very large amount of power is generated when it compared with conventional fuel (fossil fuel). Hydrogen is also used as a fuel in various energy convertors systems. Hydrogen is the most ideal and environment-friendly fuel because of its high efficiency and non-polluting in nature [171,172]. During the combustion, it is not producing any carbon products (carbon-free emission). The hydrogen storage capacity of $CoAl_2O_4$ electrodes was evaluated and access by chronopotentiometry method. It was clear that the $CoAl_2O_4$ nanostructure electrode shows good hydrogen storage capacity [171]. Due to the difficulty of storage of high-pressure gaseous hydrogen and liquid hydrogen, solid-state metal hydride hydrogen system was developed and used because of its high volumetric storage capacity. These stationary metal hydride systems have a low cost. Endo et al. showed that the hydrogen storage capacity of Ti–Fe based alloy tank was higher and mostly used for storage application because of its high absorption, desorption and heat exchange rate [173]. Another technique for hydrogen storage in the porous material is the electrochemical method. During this, electrochemical decomposition of an aqueous solution takes place and generated hydrogen is adsorbed on a material surface. Different nanostructured material such as Graphene, CNT, different oxide, metal sulfides, and hydride compounds was mostly for electrochemical hydrogen storage. Gholami and Niasari studied the CuO/Al_2O_3 nanocomposite material for hydrogen storage and they recommended that this material is cheap and having high hydrogen storage capacity. It was found that as copper to aluminum ratio was increased, hydrogen storage capacity was also increased with morphology changes and band gap [172]. Different nanoparticle and nanocomposite used for electrochemical hydrogen storage and their storage capacities are different from each other [173–177].

Sangsefidi et al. investigated the hydrogen storage capacity of Cuo-CeO_2 nanocomposites by chronopotentiometry method. They found that various parameters such as a source of cupper, temperature and time affect the morphology, particle size, and simultaneous hydrogen storage capacity. They concluded that this nanocomposite is having maximum hydrogen storage capacity with maximum discharge capacity of 2450 mA h/g after 20 cycles and most suitable for electrochemical hydrogen storage. The characterization of nanocomposites was done by SEM, X-ray diffraction (XRD), transmission electron microscope (TEM) and Fourier transform infrared spectroscopy (FT-IR) [173–175]. Thermal decomposition process was used for synthesization of $ZnAl_2O_4$ by adding green tea as precipitating means. This process widely used because of low cost, very rapid and mostly used for the preparation of nanostructured oxide material. Hydrogen storage capacity of $ZnAl_2O_4$ nanoparticle was increased using cationic, anionic and polymeric surfactants [175]. Zn_2GeO_4/graphene nanocomposite has high hydrogen storage capacity during the electrochemical reaction at room temperature than the Zn_2GeO_4 nanoparticle and

discharge capacity is still above 2695 mA h/g after 29 cycles [176]. Another nanocomposite material Co_3O_4–CeO_2 was used for evaluation of electrochemical hydrogen storage capacity. The result shows that this nanocomposite material has high hydrogen storage capacity and the maximum discharge capacity was 5200 mA h/g after 20 cycles [177]. Mn_2O_3 impurity causes the hydrogen storage capacity of MnO_2–CeO_2 nanocomposite was increased by the creation of new sites for hydrogen storage during the charging and discharging process of the working electrode [178]. Multi-walled carbon nanotubes are primarily used for hydrogen storage. With the addition of $Dy_3Fe_5O_{12}$ (DFO) nanoparticles, the electrochemical hydrogen storage capacity was increased from 420 mA h/g to 1000 mA h/g after 15 cycles [179]. $Sr_3Al_2O_6$ nanostructured material also shows a high hydrogen storage capacity with discharge capacity of 2500 mA h/g after 15 cycles and efficiency of charging and discharging would be 70% [180]. Electrochemical hydrogen storage capacity of $NiAl_2O_4$/NiO nanostructure material is improved by adding TiO_2, graphene, and SiO_2 nanoparticle. These different nanoparticles have a very unique structure which responsible for improved hydrogen storage capacity of host material [181]. Size of the nanoparticle is also main aspect when hydrogen storage capacity of different alloys is evaluated. During the investigation, it was found that Zn_2SnO_4 nanoparticle also shows a good electrochemical hydrogen storage capacity at room temperature [182]. Nanostructure material is used in many energy-related application areas such as hydrogen storage, catalysis, and batteries [191–198]. Hydrogen absorption ability and capacity are depending on nanoalloy or particle size and confinement. It was found that small size Pd–Pt nanoparticles are confined in carbon matrix and surrounded by graphite layer avoiding hydrogen absorption and large Pd–Pt particle size (more than 50 nm) cause hydrogen absorption by formation of metal hydride [192]. Hydrogen absorption ability of Pd–Ni alloy was strongly depending on chemical composition and Ni content [193].

This study focuses on the effect of diffusible hydrogen in the mechanical properties of AHSS and changes in the microstructure of the material. Mechanisms which are responsible for crack initiation, crack growth, fracture initiation and failure of material will be discussed broadly. Simultaneously prevention activities such as the effect of providing coatings (graphene, niobium, and amorphous material) above the base material, providing carbon or nitrogen diffusion layer and alloying of titanium and aluminum are explained.

Advanced high strength steel (AHSS)

Dual phase (DP) steels

DP steels are coming under the category of first-generation AHSS. Initial research started in DP steels in early 1980 [40]. This first generation AHSS have excellent mechanical properties (strength and ductility) when compared to conventional steels. Also, the production of these steels is easy. The only limitation that they have is poor formability [38,39]. The microstructure of DP steel consists of two-phase, ferrite and martensite which is shown in Fig. 2. Ferrite is having a darker

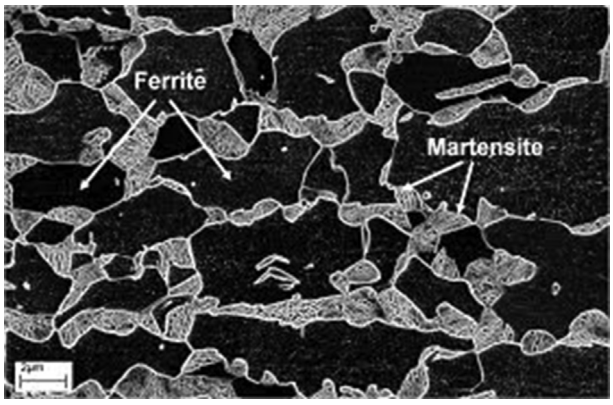

Fig. 2 – DP steel comprises of ferrite and martensite structure where black region represent ferrite and bright (light) portion represent martensite [42].

area with soft matrix whereas martensite is having light-colored small islands, which is spread along the grain boundaries of ferrite. A common method for production of DP steels is cold rolling followed by annealing and quenching [42]. If annealing temperature is high then austenite fraction in the matrix also high and this austenite transforms into martensite during the quenching process. This DP steel is having good strength because of the strength of DP steel is depends on the volume fraction of the martensite [43].

Ferrite matrix availability which is soft in nature, responsible for good formability in DP steels. While martensite which is available in grain boundaries provide good strength. This combined property of DP steels is widely used in the automotive and construction industry for the production of components [46]. Cost efficiency of DP steels is very good and encourages the industries to use in the various applications. Tensile strength and formability of DP steels may vary depending upon the carbon percentage available in DP steels, percentage of other alloying element and volume fraction of martensite in DP steels. Sometimes zinc coating is also performed above the DP steels to resist it from corrosion and it is performed by galvanization process [47]. Cooling rate and soaking time change the mechanical properties of DP steels during galvanization process. Literature also revealed that if Cr and Mo were added in correct proportion in DP steels then mechanical properties remain the same during the galvanization process [1].

TRIP steels

This steel is also coming under the categories of first-generation AHSS. TRIP steels are having a mixed microstructure or mixed phases comprises of ferrite, retained austenite, bainite and martensite as shown in Fig. 3. In microstructure, small islands of austenite were dispersed in ferrite matrix and martensite also available [48].

Two techniques available for manufacturing or processing of TRIP steels are hot rolling and cold rolling. In case of hot rolling, the process starts from the fully austenitic region and after finish rolling, controlled cooling is performed. During the cooling process, ferrite formation starts and carbon

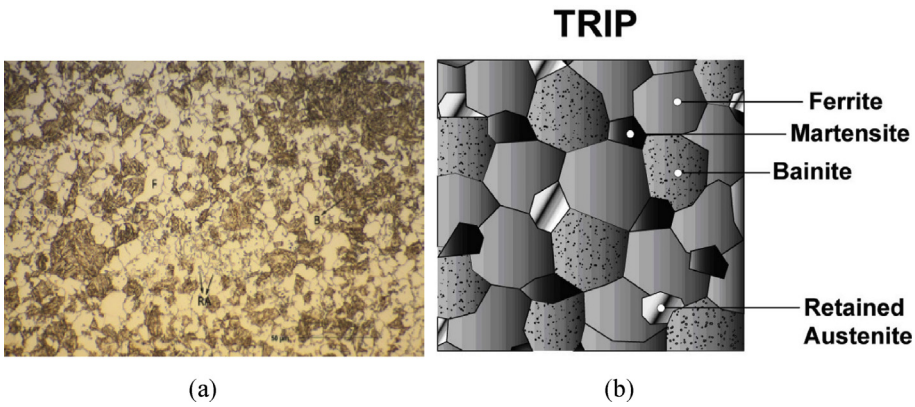

Fig. 3 – TRIP steel microstructure where F-ferrite, B-bainite and RA-retained austenite (a) [11] and (b) [155].

concentration on remaining austenite increases because austenite is having higher carbon solubility than ferrite. After the cooling process, austenite converts into bainite and again small islands of austenite increases in the matrix.

Cold rolling of TRIP steels starts from mixed matrix region comprises of ferrite and austenite microstructure. During the process, steel is heated to form a two-phase or mixed microstructure of ferrite and austenite. Sudden cooling of that mixed-phase perform to avoid the formation of intercritical of ferrite or bainite and quenching operation is done at low temperature which is also called isothermal bainitic region [49]. During this process, some austenite transforms into bainite and remaining austenite enriches due to carbon content responsible for stabilization of austenite at room temperature. Thinner steel sheets produced very effectively by using cold rolling operation. Grain size is improved and refined due to recrystallization happen during the annealing operation [50].

As TRIP steels are deformed during the process, the hard martensite dispersed in the soft ferrite matrix and retained austenite changes to martensite producing high strain hardening rate. This strain hardening rate is very high in TRIP steels as compared to conventional steels. So high strain hardening effect, good mechanical strength, and ductility provide good energy absorption ability to TRIP steels and suitable for structural and construction of complex shape, longitudinal and cross member and bumper reinforcement [51]. These steels are having good mechanical strength and formability property which inspire the various automobile bodies and construction industries.

Complex phase steels

Complex phase steels and TRIP steels both are having similar microstructure. The only difference is that the CP steels contain less retained austenite and sometimes no retained austenite is shown in the microstructure. From microstructure examination, it was found that the CP steels contain precipitates with ferrite which are having a fine microstructure and hard phase available in large volume. The hard phase of martensite and bainite with precipitates hardening help to increase the strength of CP steels. Also, by adding some element such as niobium, titanium, and vanadium to normal alloying element, precipitate hardening of these steels are taking place and mechanical properties are get improved [60]. CP steels are having high mechanical strength a range from 800 to 1000 MPa with lower alloy percentage and due to this weldability gets improved at a lower cost [59].

TWIP steels

These are the second generation AHSS. From microstructure examination, it was found that the TWIP steels are having a wholly austenitic microstructure which is dispersed in the matrix (Fig. 4). This is due to high manganese content availability in TWIP steel and sometimes more than 15 percentages of manganese are available in the matrix. Some other alloying elements such as carbon, silicon, aluminum are also available in high quantity. Carbon is responsible for stabilization of austenite at room temperature [52]. Aluminum is also responsible for stabilization of austenite and increasing the stacking fault energy (SFE). Also, carbon, Aluminium, and silicon are providing strength by solid solution strengthening.

Manufacturing techniques for TWIP steels are the same as other AHSS materials such as rolling, pressing. From the literature, it was found that these steels are having low SFE which facilitates the deformation twinning and responsible for the production of TWIP steels through strain hardening which has high mechanical strength and ductility [1,53]. This combined properties of TWIP steels is very much desirable in automotive or auto-industries, and safety component manufacturing having complex shapes such as bumper and pillars [51]. But in automotive industries, TWIP steels have not got as much recognition as other AHSS [53].

Strain hardening mechanism comprises of dislocation guide and deformation twinning processes [54–56]. At the time of straining, twins are continuously generated in the microstructure. Grains are divided by these twins with twin boundaries which provide a barrier for dislocation motion [57]. This is called Hall-Petch effect, responsible for high strain hardening and gives good strength and ductility combination to TWIP steels. During strain hardening these twins are continuously formed, grain size refined thus increasing the mechanical strength due to straining effect [58].

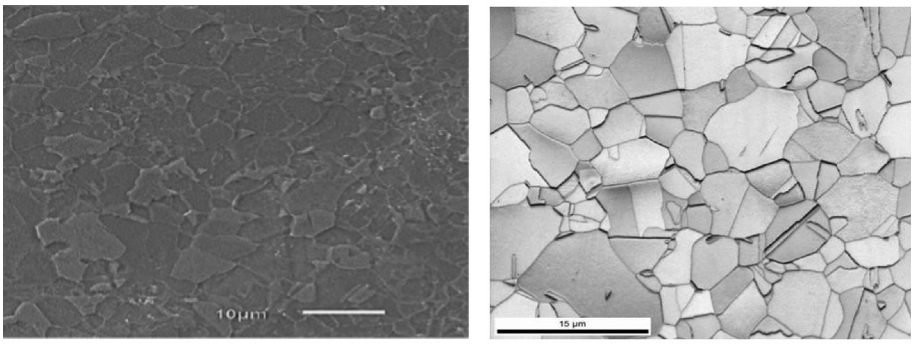

Fig. 4 – Microstructure of TWIP steel (a) [1] and (b) [155].

Q&P steels

Quenching and partitioning steels (Q&P) comes under the category of third-generation AHSS. These Q&P steels are strongest among all AHSS and give a good combination of strength and ductility among all conventional and advanced steels. This shows a good attraction to car industries where high strength is required without any increase in weight and size. Other areas where Q&P steels are used like the ship manufacturing industry, construction industries, and aircraft components [44,45].

Mechanism

If hydrogen is available in large quantity at the crack tip, then initially this hydrogen molecule has to dissociate in the hydrogen atom and adsorbs at the crack tip. In case of internal hydrogen embrittlement (IHE), solute hydrogen atom adsorbs at internal crack tip location. Hydrogen can be trapped at various locations such as at interstitial lattice site, precipitate, inclusion, grain boundaries, and dislocation cores. The schematic representation of hydrogen at the interstitial site and trapped hydrogen is shown in Fig. 5.

Literature suggested that the transports of hydrogen from its original position to a new position within metal or alloy is a complex phenomenon. Excess hydrogen causes transport of hydrogen atoms are taken place in a simple manner. Several locations where the presence of hydrogen atoms is responsible for crack growth and fracture initiation are shown in Fig. 6. Various mechanisms available for hydrogen propagation inside the materials, causes of degradation and complete failure of the material are HEDE, HELP, AIDE, HEMP, MF and HAM. Sometimes a combination of these mechanisms is also responsible for a complete failure of the material. These various mechanisms are described below.

Hydrogen enhanced decohesion mechanism (HEDE)

In 1959, Troiano was the first who introduced and explained this mechanism. This mechanism is very simple and widely accepted among the other mechanism. If the interatomic strength of atoms is reduced due to the presence of hydrogen atom at the crack tip and brittle failure (cleavage) occurs then failure causes of the mechanism is called the HEDE. This happened due to the surface energy of the material is reduced and fracture occurs below its working stress. In this mechanism, if the specimen is in the hydrogen atmosphere and hydrogen atoms are available in large quantity then hydrogen 1s electron reaches to the 3d cell of the iron atom, reducing the interatomic strength of the parent material and after some time fracture occurs at low load or less working stress [8,13,15,17,20,21,138,139]. Hydrogen damage sites are located at some distance from crack tip where the maximum tensile stress is applied [15]. This maximum acting tensile stress is greater than the cohesive strength of the material. When critical crack tip opening displacement (CTOP) is reached then the decohesion takes place. This HEDE mechanism is very much applied in internal hydrogen embrittlement as well as external hydrogen embrittlement. Fig. 7 represents the HEDE mechanism in which hydrogen initially accumulated in lattice structure and it reduces the interatomic bond strength of atom. This decohesion of atoms are generally occurs at crack tip and location of maximum hydrostatic stress area due to adsorbed hydrogen. It also occurs at particle matrix interfaces. If hydrogen is accumulated in grain boundary near the crack tip and trapped at the specific area then decohesion may take place due to the effect of hydrogen and impurities inside the metal matrix.

Hydrogen Enhanced Local Plasticity Model (HELP)

Hydrogen Enhanced Local Plasticity Model (HELP) was first suggested by Beachem in the year of 1972. He proposed that hydrogen atoms excite the dislocation process near the hydrogen zone and the localized plastic deformation takes place which supports the sub-critical crack growth in the material with ductile fracture when it is seen on the macroscopic scale (Beachem, 1972). In this mechanism, the hydrogen atoms accumulated near the crack tip zone and the resistance for dislocation motion had decreased so the dislocation mobility increased and this dislocation mobility behaves as carriers of plastic deformation in a metal lattice [14,140]. Local dislocation movement is possible at the low level of stress due to hydrogen because of local drop-in yield stress. This means that embrittled material shows local plastic deformation at fracture surface and slip bands at the crack tip zone [15]. Still, it was found that the connection

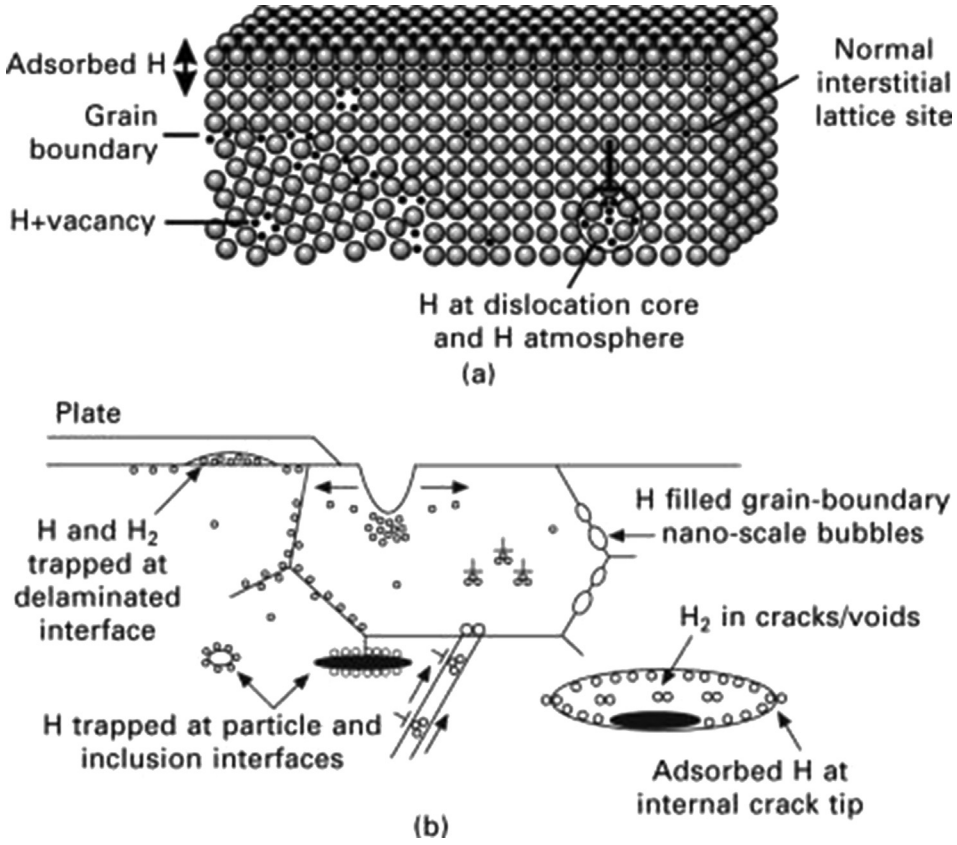

Fig. 5 – Schematic representation of hydrogen at interstitial lattice site and trapped location at (a) atomic scale and (b) microscopic scale [19].

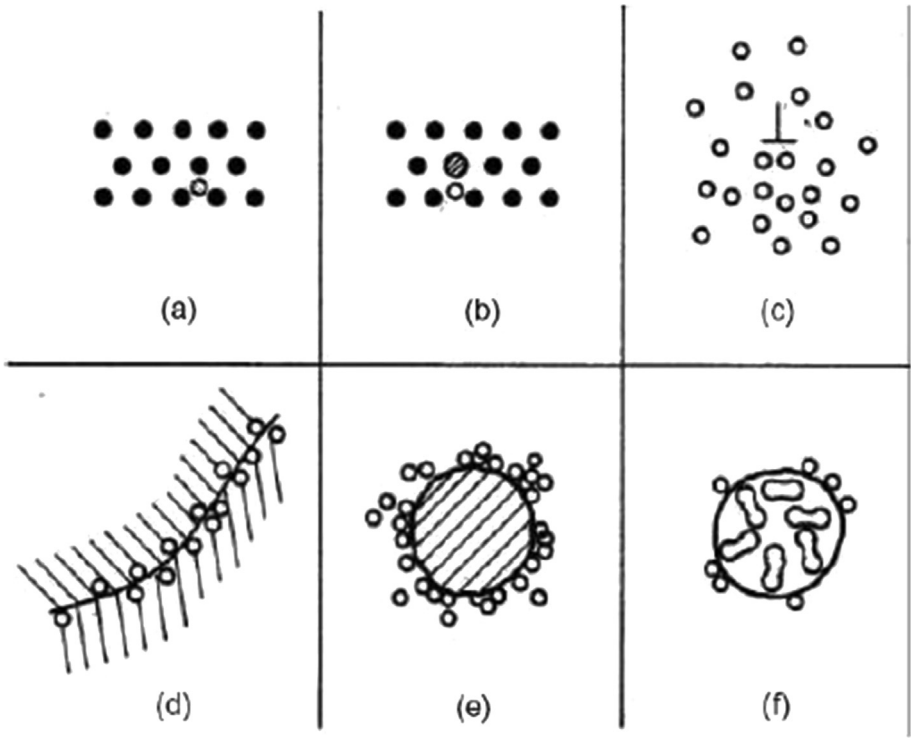

Fig. 6 – Various location where hydrogen atoms are presented in microstructure are (a) solid solution; (b) solute–hydrogen pair; (c) dislocation atmosphere; (d) grain boundary accumulation; (e) particle-matrix interface accumulation; (f) void containing recombined hydrogen [153].

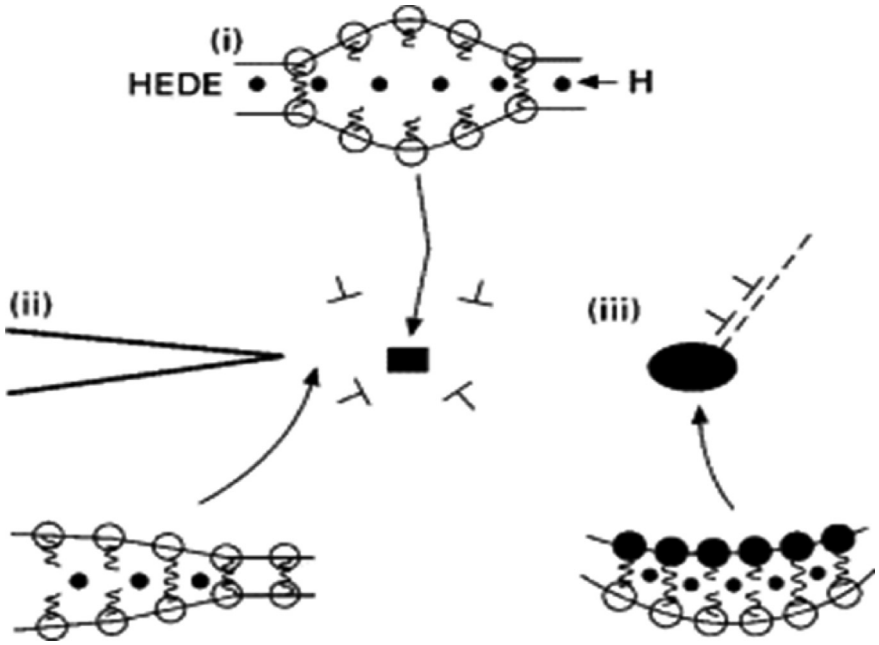

Fig. 7 – Schematic diagrams illustrating the HEDE mechanism, involving tensile separation of atoms owing to weakening of interatomic bonds by (i) hydrogen in the lattice (ii) adsorbed hydrogen and (iii). hydrogen at particle–matrix interfaces [151].

between planned and proposed HELP model and real embrittlement mechanism is unclear [15]. Fracture modes such as intergranular, transgranular and quasi-cleavage have been seen in microstructure examination and it depends on the amount of hydrogen available in the surrounding (hydrogen atmosphere) and crack tip stress intensity. Dislocation motion activation energy is diminished due to the large hydrogen atom availability and its effect [8,21,24,26,141–143]. More plastic changes are seen by fractographic imaging with diminishing in macroscopic ductility. Material having FCC, HCP and BCC structure may be affected by this HELP mechanism [19]. Fig. 8 represent the HELP mechanism which involves the microvoid nucleation, their growth and coalescence of these voids with simultaneous dislocation motion in the region of high hydrogen concentration area and localized plasticity occurs in these stressed areas due to the effect of hydrogen and crack growth took place.

Adsorption-induced dislocation emission (AIDE)

This AIDE is a combination of two mechanisms HEDE and HELP. Adsorptions of hydrogen atoms are taking place at the crack tip which is a region of high-stress concentration. This adsorbed hydrogen goes inside the lattice from the crack tip and reduces the interatomic strength of the material by HEDE mechanism and dislocation motion is possible with more plastic deformation by slip and microvoid formation at the crack tip by HELP mechanism [138,140]. Nucleation of crack

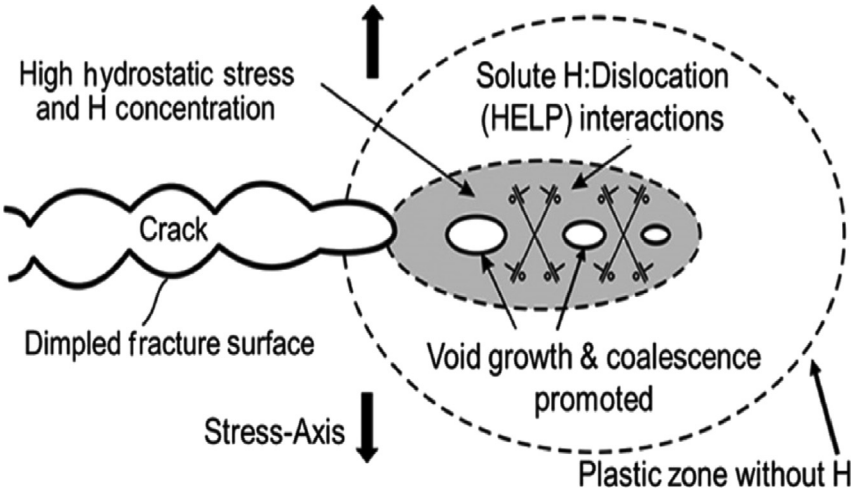

Fig. 8 – Schematic diagram explaining the HELP mechanism, comprising microvoid nucleation, growth and coalescence of these microvoids, plasticization in localized area due to the effect of hydrogen concentration and dislocation motion [151].

and its growth takes place due to the combined effect of decohesion and dislocation emission and fracture occurred at the crack tip by slip and micro-void coalescence (MVC). In a material like Fe, Ni and Ti, a high percentage of adsorbed hydrogen have detected to support AIDE mechanism [8,21,24,144,145,150]. Fig. 9 represents the AIDE mechanism which explains the crack initiation occurs at stressed region due to decohesion mechanism and dislocation motion possible due to HELP mechanism with simultaneous voids coalescence at plastic zone due to hydrogen concentration. Absorption of hydrogen is responsible for reducing the interatomic bond strength and supports the dislocation emission from the crack tip. This dislocation emission promotes the crack growth and coalescence of cracks with voids responsible for producing dimple on the fracture surface.

Hydrogen Enhanced Macroscopic Ductility (HEMP)

It is also called as hydrogen enhanced macroscopic plasticity model. If hydrogen atoms are available in large quantity and the whole specimen is surrounded by hydrogen then this hydrogen causes mechanical properties of a material are changed and yield strength of the material gets reduced due to the diffusion of hydrogen and solid solution softening by a hydrogen atom. It was also found out that plasticization of the whole specimen occurs with macroscopic enhancement in plasticity due to yielding of material. This reduction in yield strength due to the presence of hydrogen atom is defined as Hydrogen Enhanced Macroscopic Ductility (HEMP). More dislocation motion is possible at this reduced yield strength with the presence of hydrogen and continues plastic deformation took place with lower functional stress-rate [146–148].

Hydrogen assisted micro-fracture mode (HAM)

Microfracture mode of the material was changed due to the presence of hydrogen and ductile to brittle fracture mode transition was took place. It was seen when the microstructure examination is done by SEM. Hydrogen charging is the main reason behind the ductility reduction of the material and fracture mode changes from cup and cone to brittle shear fracture mode at ultimate tensile strength. The high percentage of hydrogen at cracking site of material is assisting the dislocation of atoms and the main reason behind the shear fracture mode. This changing of microfracture mode due to the effect of hydrogen is called Hydrogen Assisted Micro-fracture (HAM) [3,146–148].

Decohesive hydrogen fracture (DHF)

This fracture mechanism is caused due to the decohesion effect facilitated by hydrogen and it is brittle in nature. When final fracture mode was seen, it was found that there is some brittle fracture initiated with the effect of hydrogen and simultaneously ductile fracture also seen in many places. This decohesive hydrogen fracture may be seen as the final fracture initiation site of the specimen [2].

Mixed fracture (MF)

It was found that fractography of the fractured specimen surface comprised of brittle fracture (fisheye) and ductile (MVC) fracture mode when it is seen in microscopy (SEM). This simply suggests that the final fracture of the specimen took place due to the combined effect of these two mentioned

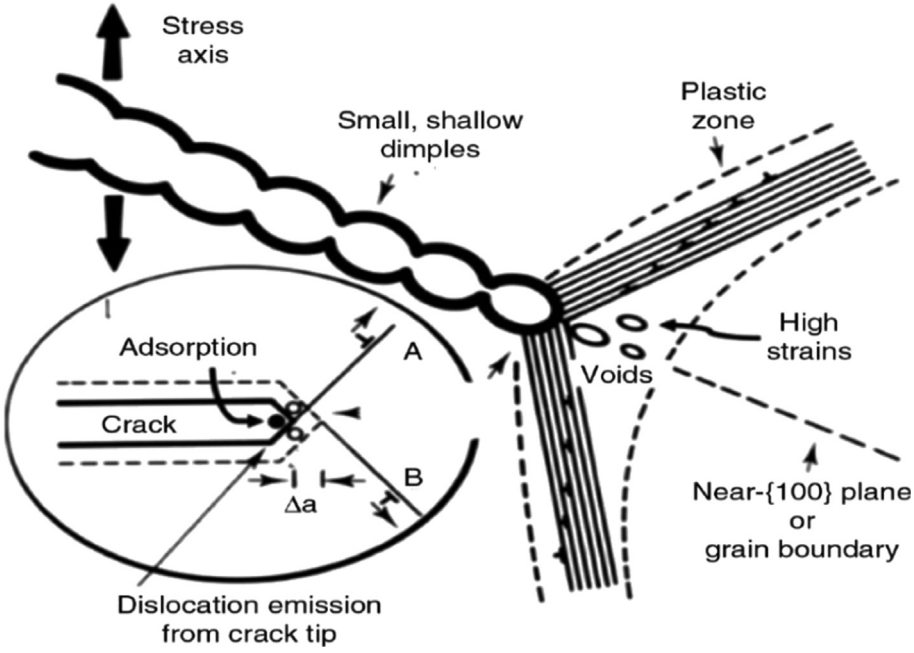

Fig. 9 – Schematic representation of adsorption-induced dislocation emission (AIDE) mechanism HEE, which comprises cracks initiation taken place at stressed area due to decohesion mechanism and slip motion from crack tip with simultaneous coalescence of these cracks and plasticization of stressed area occurs due to hydrogen accumulation and concentration [19,152].

micro-fracture mechanisms. Fish eyes are commenced at the innermost area of specimen and growth takes place in a radial direction until they come in contact with micro-void coalescence which is ductile in nature. Also, these fish eyes are enclosed by micro-void coalescence fracture. This fracture mechanism where two different fracture modes are competing with each other is called the mixed fractured mode. These fish eyes were generated due to the effect of hydrogen and hydrogen fracture mechanism [3,24].

Hydrogen assisted micro void coalescence (HDMC)

Micro-void coalescence (MVC) is a ductile fracture mechanism. The numbers of stages from where MVC crack generation and propagation takes place are void nucleation, void growth, void coalescence and crack extension and at last breaking of remaining ligament by shear. Dislocation and local plastic deformation take place due to the effect of hydrogen. The crack growth takes place in a zig-zag pattern by connecting the voids present in the crack propagation direction. Due to the effect of hydrogen MVC dimple produced but they acquire poor ductility. The final fracture appears as a result of shear stress so parabolic shallow shear dimple presented. At the edge of the specimen, brittle intergranular fractures have seen due to the effect of hydrogen. This is called hydrogen assisted micro-void coalescence (HDMC). So it was clear that the effect of hydrogen on the ductile MVC process. Sometime fisheyes (brittle) are also found in final fracture or rupture propagation region which acquires MVC shear dimple and these shear dimples are covered by MVC dimples [24,149,150]. As these micro-void dimples have coalesced, the amount of hydrogen concentration increases and when it reaches to the critical amount then the final brittle fracture of the specimen takes place in the hydrogen-rich region and creating fish eye structure [14].

Effect of hydrogen in dual phase steel

Effect of hydrogen in DP steels is characterized on the basis of strength degradation, fractography and microstructure examination or behaviour. Several authors are worked to explain the effect of hydrogen on mechanical and microstructural changes of DP steel and causes of this degradation [61–72].

Mechanical properties degradation

For mechanical properties degradation and examination, linearly increasing stress test (LIST) and slow stress rate test (SSRT) have conducted. Properties such as yield strength, ultimate tensile strength, percentage elongation and percentage reduction in the area have calculated to characterize the effect of hydrogen in dual-phase steels [62–65,67–69,72].

LIST is a direct stress measurement technique in which cracking begins due to the effect of hydrogen. LIST is also called as load control testing. On the other hand, SSRT is a strain rate control testing technique in which the strain is applied and it increased up to fracture of the material. The only difference between LIST and SSRT was that LIST technique gives quick result whereas SSRT technique requires more time to perform testing and getting the result [2]. If the material is failed due to the effect of HE then the following things must be taken in consideration (i) threshold stress below which no cracking in material takes place, (ii) reduction in ductility of the material and (iii) hydrogen embrittlement index (HEI). Reduction in ductility was calculated by total elongation (e) and the total reduction in area (R_A%) of material at fracture [1].

$$e = \frac{l_{f-l_i}}{l_i} \times 100\% \tag{1}$$

$$R_A\% = \frac{A_i - A_f}{A_i} \times 100\% \tag{2}$$

Where notations are usual meaning, l_f is the final gauge length and l_i is the initial gauge length of the fracture specimen and A_i is the initial area and A_f is the final area of the fractured specimen.

The hydrogen embrittlement index (HEI) (I) was calculated by Ref. [73].

$$I = \frac{R_{A,air} - R_{A,H}}{R_{A,\ air}} \times 100\% \tag{3}$$

Where $R_{A,air}$ is the reduction in area in air and $R_{A,H}$ is the reduction in area in the hydrogen charged atmosphere. The value of HEI (I) is varying between 0 and 100%. When material has no embrittlement then value of I is 0 and when the material having purely hydrogen embrittlement means having no (zero) ductility then value of I is 100%.

Loidl and Kolk (2012) explained the effect of hydrogen in mechanical properties of various DP steels such as DP 1000 and DP 1200. During the examination, they found that the yield strength and ultimate tensile strength have not changed considerably due to the effect of hydrogen but ductility of the material was changed significantly. It was found that the ductility of DP 1000 was changed from 12% to 7% and for DP 1200 steel total elongation was changed from 9% to 5%. The HE index for those steel was 40% and 47% respectively. This value is higher than those of complex phase and martensitic steel having similar strength and same operating condition [73]. Begic Hadzipasic also explained the effect of hydrogen charging on the microstructure of some advanced high strength steel material like DP and TRIP steels. They also concluded from the examination that the effect of hydrogen on mechanical properties was negligible but the percentage elongation had reduced considerably. Percentage elongation has changed from 64% to 26% and HEI was 59%. From this, it was indicated that DP steels have very low resistance for hydrogen diffusion and highly susceptible to hydrogen embrittlement. Causes of this susceptibility were the presence of carbon and martensitic islands in DP steels microstructure [68]. TDS analysis was formed for hydrogen content measurement [189,190].

Further studies of the effect of hydrogen in mechanical properties of DP steel were carried out by Koyama et al. (2014) and Depover (2016). They found that the Ductility of the material has changed considerably. Parameters which influence the diffusion of hydrogen in DP steels are the testing speed and time for hydrogen charging. It was proposed from

literature survey that lowers the testing speed, more changes of hydrogen atoms to diffuse inside the material due to long diffusion time and further suggested that material susceptibility to HE is also increased [10,76].

Fractography examination

Fractography of DP steel revealed that it changes from ductile dimples to brittle transgranular cleavage like fracture with the effect of hydrogen in DP steels as suggested by Davies [74]. His observation was that the cleavage formation starts from the large martensite region in DP steels and sometimes it starts from the interface between the hard martensite and ferrite region. The propagation of these cracks takes place through softer ferrite. Stress concentration is the main reason behind the crack initiation and it starts due to strain hardening rate effect of the martensite and ferrite. Crack initiation and propagation are taking place due to the effect of hydrogen and this is facilitated by decohesion mechanism and dislocation motion.

Sun et al. studied the effect of cathodic charging on DP steels. They found that martensitic, ferrite interface and lath martensite are widened due to the effect of hydrogen or hydrogen charging. This widening effect increases at higher current density. Micro-cracks were generated at the interface between lath boundaries of martensite, interface widened and changed from smooth to transgranular form [75].

Effect of hydrogen on DP steel was characterized by various technologies such as scanning electron microscopy (SEM) and electron backscattered diffraction technique (EBSD) [71]. During the investigation, it was found that crack initiation starts from the martensitic region and their growth takes place along the martensitic and ferrite interface region. The critical strain reduced due to the effect of hydrogen decohesion mechanism and when this critical strain will be reached then decohesion facilitated cracking takes place.

Depover et al. were explained that the fracture surface changes from ductile dimples to brittle transgranular cleavage due to the hydrogen effect [10,76]. Their observation said that the testing speed plays an important role in hydrogen charging and hydrogen-related failure. During experimentation, if tensile testing was performed simultaneously with cathodic charging then they found that the lower the testing speed, more changes of hydrogen atoms to diffused inside the material and changed the microstructure of DP steels because sufficient time provided for a hydrogen atom to diffuse. They performed testing at 5 mm/min and 0.5 mm/min and they found that at testing speed of 0.5 mm/min, fracture surface appears as brittle transgranular where hydrogen concentration was large. They also suggested that at lower testing speed, the dislocation density of a material is increased significantly and this increases in the hydrogen diffusion coefficient of the material so more changes of a hydrogen atom in the central part of the specimen.

Microstructure examination

Microstructure plays an important part during the investigation of the influence of hydrogen in DP steels. Various authors investigated and suggested that the martensite is the main reason behind the HE of DP steels. Cracks were initiated in martensite region or martensite and ferrite interface region [68,74,75]. The effect of martensite percentage on hydrogen embrittlement of DP steels was studied experimentally. Various samples were quenched in brine solution after a salt bath at a distinct temperature range to produce DP steels having different ferrite and martensite constituent. The martensite percentage may vary between 5% and 45%. As martensite content increases, the grain size of ferrite reduces and tensile strength of material gets increase linearly but HE susceptibility of DP steels does not increase linearly. To examine this, the ratio of elongation after hydrogen charging to the uncharged condition was evaluated. During examination they found that microstructure was influenced by martensite and their embrittlement effect divided into different categories: (i) no effect of HE up to 10% of martensite, (ii) between 10% and 30%, susceptibility of HE increases and (iii) more than 30% of martensite, embrittlement effect was the same as earlier. Morphological variation examination is very much desirable for a complete understanding of martensite content in HE. Morphology of DP steels was changed as martensite percentage was increased and the grain size of ferrite was reduced. Martensite percentage facilitates the path for crack propagation so HE susceptibility is increased. Davies suggested that the tempering of DP steel reduce the susceptibility of HE so tempering temperature plays an important role to reduce HE susceptibility. At 500 °C tempering temperature, percentage changes in elongation were same as of uncharged specimen. It was also found that the yield strength of material increases without changing in the ultimate tensile strength of the material [74]. Inclusions are also responsible for hydrogen-induced crack initiation. These inclusions such as oxides, oxisulfides, and oxicarbides behave like an irreversible trap and responsible for HE susceptibility of DP steel and participate in crack initiation [68,84].

Effect of hydrogen in TRIP steel

The literature said that the hard microstructure of martensite is more susceptible to the hydrogen embrittlement [77,78]. During the production of TRIP steels, austenite is converted into martensite and excess hydrogen releases during this transformation process and get diffused into martensite. If there is certain defined mobility of hydrogen atom then crack propagates from crack tip due to the accumulation of hydrogen at the crack tip and this is called as hydrogen supported crack propagation [78]. Further studies are suggesting that due to high hydrogen percentage in TRIP steel, ductility of the material reduces significantly without any fracture behavior changes [79].

Mechanical properties degradation

SSRT testing was performed in TRIP 800 steel with different hydrogen percentage and it was found that the percentage change in elongation is reduced as hydrogen content increases [65]. During the examination, it was found that a critical amount of hydrogen is required for hydrogen-related failure and when this critical hydrogen percentage reaches

then the material is highly susceptible to HE. For TRIP 800 steels, the critical hydrogen percentage required was 2.5 wt ppm and hydrogen embrittlement index for that material was 27%. A similar type of observation was found by Ryu et al. (2012) where the reduction in ductility was recorded [67]. TRIP 700 steel was also affected by the hydrogen influence and observation said that the percentage of elongation was changed from 30% to 10% with HEI (I) was 66%. This calculated HE index was higher than the other AHSS material such as CP, DP and MS steels when performed in similar operating condition [73].

Fractography examination

Fractography of material changes from ductile dimples to brittle topographic features with degradation in mechanical properties of TRIP steels due to the increase in hydrogen content. The final fracture surface of the material becomes highly brittle due to the percentage increase in hydrogen content. Comparison between charged and uncharged specimen are studied and proposed that uncharged specimen is purely failed by ductile manner whereas in hydrogen charged condition specimen shows brittle fracture feature [65]. They also observed that the cracking initiates from the hard-martensitic region and further propagates in ferrite soft region. Sojka et al. investigated the effect of hydrogen on the fracture surface of TRIP 800 C–Mn–Si steels at different current densities. They observed that at 15 mA/cm^2 current density, fracture surface comprises of both ductile and cleavage (transgranular). At high current density (30 mA/cm^2), transgranular cleavage observed entirely in fracture surface [80]. The hard-martensitic region plays an important role in crack initiation. TRIP steel is highly susceptible for HE because of large austenite region. As literature told that austenite has high hydrogen solubility and low diffusivity for hydrogen, austenite enriches by hydrogen and when the transformation process takes place then the martensite enriched with hydrogen, cracked instantly [65]. This mechanism of crack initiation was kept by various researchers [79,81]. Laureys et al. were studied this mechanism of crack initiation of TRIP steels by EBSD technique. They observed that the crack originates between MS region by decohesion mechanism and propagates through either ferrite, martensite interface or through the matrix. A similar observation was taken by Zhu and his colleagues during hydrogen pressurized cracking [82,83].

Microstructure examination

The microstructure plays an important role in TRIP steel for investigation of hydrogen embrittlement. Two microstructures (austenite and martensite islands) are observed during the examination of TRIP steels by SEM. Other elements which can affect the HE behavior of TRIP steel are alloying and composition constituents along with manufacturing methods. TRIP steels are less sensitive to HE on austenite state, as long as it converted into martensite during the transformation process. This martensite phase brittle in nature and responsible for the final fracture of TRIP steels. A lot of researchers observed the HE features of TRIP steel when it transformed into martensite from austenite on the straining process [65,73,79,85,86]. Plastic deformation takes place during this transformation process and trapping of hydrogen in many places because austenite has large solubility for the hydrogen atom. The deformation-induced transformation has reduced the trap binding energy, allowing increased mobility of the hydrogen atom and causes mechanical properties degradation of TRIP steels [67]. The dislocation distribution effect on HE of TRIP steels was investigated by Ronevich [86]. By TDS analysis it was found that dislocation provides the trapping site for hydrogen diffusion in TRIP steel. To explain this 5% prestraining was applied in TRIP steels at a distinct temperature of 253, 296 and 373 K for martensitic phase or structure. During the examination, it was found that at 5% prestrained of TRIP steel at a temperature of 253 and 296 K, clustering of dislocation took place with transformed martensite whereas TRIP steel prestrained 5% at a temperature of 373 K, dislocations were distributed uniformly and offers improved resistance for HE. Effect of the alloying elements on HE effect of TRIP steel was investigated by HOJO et al. [87]. Effects of the alloying elements such as Al, Mo, and Nb in high strength TRIP steels made for automotive applications were investigated. They found that stable austenite percentage in TRIP steel due to the effect of these alloying elements increase. After hydrogen charging, the percentage of hydrogen concentration increased with increased in volume of retained austenite because hydrogen was trapped in retained austenite or austenite-ferrite interface matrix. The typical trapping sides such as grain boundaries, dislocation was suppressed so the effect of hydrogen in TRIP steel with the addition of alloys reduced [87]. Zhu et al. investigated and explained the cryogenic tempering treatment effect on HE of TRIP steel. They used the SSRT technique for mechanical properties evaluation, EBSD technique for microstructure assessment and crack origination and fractured surface examination by SEM technique. They concluded that cryogenic tempering (CT) treatment causing HE resistance of TRIP steel increases with less reduction in ductility and low brittle fracture features. This cryogenic temperature leads to an increase in retained austenite stability, reduction in martensite and lowers the hydrogen content which causes a reduction in crack initiation and propagation. The CT treatment possesses a reduction in dislocation clustering due to the continuous and uniform distribution of dislocation. This causes HE resistance of TRIP steel was increased. Nonmetallic inclusions were the preferential site for HE in TRIP steel because hydrogen concentration was high in these inclusion sites [68,80].

Effect of hydrogen in TWIP steels

Mechanical properties degradation

Mechanical properties degradation in TWIP steels due to the effect of hydrogen was inconsistent. Some authors were found that there is a considerable degradation in mechanical properties whereas some examined and said that little or no influence of hydrogen in properties [69,79,86,88,89,91]. TWIP steels are generally failed by Hydrogen delayed fracture (HDF).

It was suggested that after adding Al in TWIP steel, susceptibility toward the HDF can be decreased [58,90]. The effect of hydrogen on Fe–18Mn-1.5Al-0.6C TWIP steel was studied by So et al. [69]. They found a very little change in mechanical properties of TWIP steel. Another observation was taken from Ronevich in 2012. During experimentation, hydrogen charging was performed on various samples of TWIP steel by varying the charging time at constant current density. The tensile test result showed that the mechanical properties such yield strength, ultimate strength and strain to failure was not changed significantly due to the effect of hydrogen when it was compared with uncharged specimens [89]. A similar observation was taken from Suh (2014) with very little changes in mechanical properties due to hydrogen diffusion and hydrogen-related fracture of TWIP steel due to the low hydrogen diffusion coefficient of austenite [92]. Reduction in mechanical properties was observed by Koyama et al. (2012, 2014). The study was performed in Fe–18Mn-0.6C TWIP steel and Fe–18Mn-1.2C TWIP steels by cathodic charging at 10 A/m^2 current density and in 3% aqueous NaCl solution containing approx. 3 g/l NH_4SCN. Tensile strength of Fe–18Mn-0.6C TWIP steel was reduced from 1200 MPa to 1010 MPa and percentage elongation was changed from 70% to 32% due to the effect of hydrogen. A similar observation was found in Fe–18Mn-1.2C TWIP steel where ultimate strength was decreased by 20% and the percentage elongation was reduced from 80% to 42% [61,63].

Fractography examination

Fractography of TWIP steels as suggested by authors are appeared wholly ductile morphology where mechanical properties were not changed significantly due to the effect of hydrogen and fracture surface showed micro-void nucleation, propagation and coalescences [79,89] and other hands, some researchers who found degradation in mechanical properties, have brittle features on fractured surface [61,63,91,93]. Fractured surface of hydrogen charged TWIP steels specimen revealed an intergranular fracture features at the boundary of a specimen or near the surface and central region still failed by ductile manner. This difference in fractography was due to maximum hydrogen atoms accumulated near the surface of the specimen and failed intergranular and this hydrogen cannot reach to the central part of the specimen so ductile dimple rupture presented in the middle portion of specimen [63]. Brittle fracture having transgranular in nature was observed in fractured surfaces examination [93]. Fractography comprises of intergranular as well as transgranular fracture features. Transgranular cracks propagated along the primary distortion twin boundaries and parallel to the secondary twinning plane. As a result of this twin-twin association, where primary deformed twins are interrupted by secondary twin boundaries, causes and responsible for transgranular fracture in TWIP steels.

Stacking fault energy (SFE) and microstructure examination

Stacking fault energy (SFE) was played an important role during transformation and plastic deformation of TWIP steels. Main factors which appeared during the plastic deformation of austenite are a transformation in martensite, twining effect, and dislocation slip or glide [1]. Chemical composition and temperature are the two factors on which SFE depends and the effect of aluminum, silicon, and manganese are maximum. Twinning has occurred during the deformation process when SFE falls within 18–50 mJ/m^2. If SFE has a low value then a martensitic transformation occurs widely and for a high value of SFE, prominent mechanism is dislocation glide [57,94–96]. From literature, it was found that hydrogen has more influence and it causes the austenite phase change into martensite so the stability of austenite could reduce and mechanical properties degraded [78,97]. These changes are due to the fact that hydrogen reduces the SFE and a simultaneous increase in stress gradient. This reduction in surface energy was reported in AISI 304 steel when the examination is done by X-ray diffraction technique with TEM [98]. Ryu et al. also explained the effect of hydrogen in SFE of TWIP steels and found that reduction in SFE due to the effect of hydrogen in Fe-0.6C–18Mn TWIP steel and austenite transforms to ε-martensite due to this reduction in SFE and more susceptible for HE [99].

Mechanical properties of TWIP steels was changed considerably due to the effect of hydrogen so material possesses toward the HE [61,63,99]. Current density plays an important role during the investigation of HE of TWIP steels. Higher the current density, more chances of the material susceptible to hydrogen embrittlement. This was seen by Koyama et al. during their investigation. During hydrogen charging at the current density of 1 A/m^2, it was found that no more changes in mechanical properties of Fe–18Mn-0.6C TWIP steel and material failed in a ductile manner. At higher current density between 3 and 10 A/m^2, it was found that mechanical properties are decreased with intergranular fracture due to the effect of hydrogen. But still, strain hardening behavior of this steel was not changed. From this study, it was concluded that the main reason for HE of these steels was a reduction in grain boundary cohesion due to hydrogen influence without significant change in strain hardening and without ε-martensite formation during the transformation process [61].

Morphology properties correlation

Morphology is basically depending on micro constituent or microstructure available in material and amount of hydrogen absorbed [156]. If these micro constituents are changed or deformed from one form to another then morphology of particular material also changed accordingly. Morphology of the fracture surface was examined by scanning electron microscopy (SEM) [157]. The study of the morphology of tensile tested fractured specimen surface is very desirable for a complete understanding of the fracture behavior of hydrogen charged specimen [158]. During SEM examination of the fractured surface, it was found that uncharged specimen was failed in a ductile manner with microvoids coalescence (MVC) fracture features. Particles which act as a microvoid initiation site found inside the void. Hydrogen charged specimen was shown a quasi-cleavage fracture surface morphology [159]. Sometimes hydrogen charged specimens were shown a microvoids coalescence of voids with a ductile fracture but at

someplace around the edge, intergranular fracture was observed [158]. If the morphology of fracture specimen changes due to the effect of hydrogen and micro constituent, then the mechanical properties are affected. Steel which having martensite in its microstructure is most likely to suffer from HE.

A case study was performed by Djukic et al. [157] to explain the morphology of fracture specimen with its mechanical properties variation. SEM technique was used to examine the fracture surface of an embrittled specimen, simultaneous fracture mode recognition and change in principal HE mechanism causing characteristic changes or modification of fractured features. They further concluded [157] that the Morphology of the fracture boiler tube was changed due to hydrogen-induced corrosion process and window type fracture feature seen in boiler tube inner wall (fireside) surface and high-temperature hydrogen attack (HTHA) was the possible mechanism to failure of boiler tube due to high hydrogen concentration in a localized area. Embrittlement took place in a localized area near window type fracture. Initially, microstructure near the fracture surface is pure ferrite and an intergranular micro-crack are seen. Ferrite and pearlite microstructure have seen from some distance from fracture edge. So due to microstructure changes, mechanical properties are also affected. In this case study [157], it was found that mechanical properties of boiler tube are reduced considerably due to HTHA fracture mechanism. Percentage of elongation changes from 26.3 to 13.2. Embrittlement index increases from 15.9 to 57.8 as shown in Table 2. Yield and ultimate tensile strength are decreased when compared with the damaged tube of opposite side. Hardness of that fractured boiler tube decreases when goes away from fracture zone as shown in Fig. 10. A mixed mode of fracture was seen in final fracture surface. Transgranular cracking and microvoid coalescence (MVC) were seen during SEM examination of the fractured surface (Fig. 11). If hydrogen concentration is more, then a final fracture occurs in brittle (intergranular (IG) or transgranular (TG)) manner and proposed mechanism is HEDE and if H concentration is less then due to coalescence microvoids, final fracture takes place and the responsible mechanism is HELP. So, it was concluded that due to microstructural changes (effect of hydrogen), morphology of fracture specimen change and mechanical properties are reduced with the simultaneous action of various mechanism [157]. Fracture morphology explained that the material was failed by the combined effect of HEDE and HELP mechanism and fracture toughness of material was reduced. HEDE causes more reduction in fracture toughness with brittle cleavage like fracture [160]. Koyama et al. also investigated and explained the HEDE and HELP mechanism on dual phase steel during electrochemical hydrogen charging. During the investigation, they found that the hydrogen assisted damage occurs when

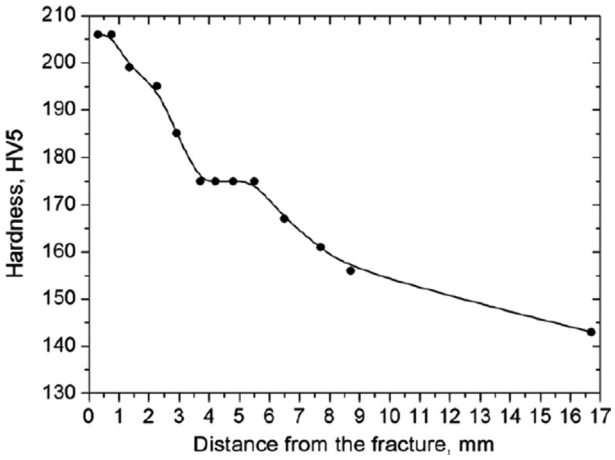

Fig. 10 – Variation of the Vickers hardness (HV5) as a function of the distance (x) from the edge of the fracture [157].

tensile test and 3-point bending test are performed. They concluded that both HEDE and HELP mechanism are responsible for micro crack initiation and propagation. IG cracking is observed in ferrite and martensite interface due to HEDE mechanism and ductile MCV features available in near subregions [161]. Different fracture mode available due to hours of hydrogen charging are ductile, mixed, brittle fracture mode and transition mode. After H charging for many hours, whole brittle fracture morphology was observed with triple-junction intergranular crack in SEM fractography and strength and elongation were reduced [162].

Precipitates were played an important role in fracture morphology change of particular material. Sometimes these precipitates act as a source of hydrogen. If precipitates are available at grain boundary these precipitates act as a hydrogen accumulator. Fine precipitates at grain cause slipping action take place by shear mechanism and simultaneously fracture mode of the material were changed with property reduction [163,164]. Due to grain boundary carbide precipitation in alloy 690, fracture toughness of material was reduced from 210 to 90 KJ/M2. So, the embrittlement effect was seen due to carbide precipitation at grain boundary [165].

Komazaki et al. studied the effect of copper precipitate particle morphology in HE behavior of copper added low carbon steel. Copper precipitated particle (ε-copper) causes copper cluster formation and these ε-copper gives more chance to hydrogen to entry in steel. Copper precipitates act as a trapping site for hydrogen and a simultaneous reduction in mechanical strength during hydrogen charging condition [166]. Precipitates in steel and alloys act as a trapping agent and their trapping capacity was evaluated by TDS method [184]. High chromium (Cr) alloying percentage in Ni–Cr–Fe alloy causes HE chances was increased. Symons explained that

Table 2 – Mechanical properties variation (boiler tube samples) [157].

Specimen	Yield strength (MPa)	Tensile strength (MPa)	Elongation (%)	Embrittlement index (%)
damaged tube, "fireside"	403	481	13.2	57.8
damaged tube, "opposite"	323	460	26.3	15.9
new tube	312	471	31.3	

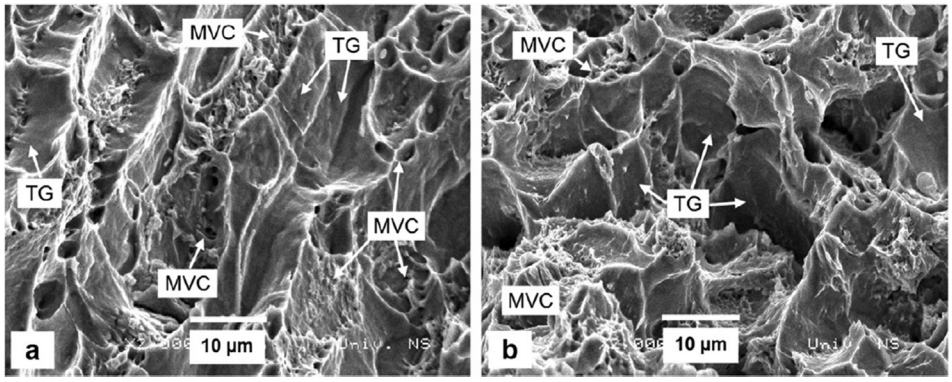

Fig. 11 – SEM micrograph of the Charpy specimens: (a) where HELP mechanism dominate (HELP > HEDE); (b) where HEDE mechanism dominate (HEDE > HELP) [157].

hydrogen causes ductility of the material was reduced in high Cr alloying, fracture morphology of alloy was changed from ductile dimple to intergranular failure with elongation at failure decreased from 53% to 14% and maximum embrittlement effect was witnessed with 26% Cr alloying [167].

Diffusible hydrogen causes mechanical properties are reduced accomplished by many researchers with final fracture mode was changed from ductile dimple to brittle cleavage formation morphology [168–170]. This diffusible hydrogen accumulates in highly stress-zone area near the crack tip, causes dislocation emission and support both crack initiation and propagation.

Preventing the HE of AHSS

AHSS materials are used in many places such as automotive components manufacturing, transportation industries, and petrochemical industries. During the operational time if hydrogen is available in the operating environment then working material comes into contact with hydrogen and embrittlement of material takes place. To reduce this, some preventive actions are required so that material cannot be affected by hydrogen and further mechanical properties of materials are not degraded by the effect of HE. There are the various methods by which the HE influence reduced such as selection of the material which is less susceptible for HE, baking operation after hydrogen diffusion, alloying of some material to parent material, coating over the base material, nitrides and oxides surface layer, providing amorphous structure layer over the base material and providing carbon diffusion layer [29,102–106]. The material surface must be cleaned and notches and irregularities are avoided because they act as a hydrogen storage agent and increase the chances of HE [100,101]. Low hydrogen plating techniques, low residual and applied stress cause chances of HE are reduced. These prevention techniques are discussed in detail below.

Material selection

High strength materials are generally susceptible to hydrogen embrittlement failure. To reduce this, the material having low ultimate strength and high resistance toward the HE are used depending upon the application. But in automotive industries, high strength is required with weight reduction. By achieving this, fuel consumption in the automobile industries is reduced. From literature, it was found that by using AHSS material in automotive application fuel consumption reduces up to 8% if the percentage of weight reduction is 10% [107]. But these AHSS materials are degraded when it comes in contact with the hydrogen environment. Some materials such as austenitic steels, aluminium, and its alloys, copper and its alloys are behaving as hydrogen resistance materials because their susceptibility to HE is low [109]. So select material which has low susceptibility toward the HE.

General methods to prevent from HE

The baking operation is performed to reduce hydrogen concentration in hydrogen charged material. Baking is a heat treatment operation in which material is heated to a suitable temperature and this temperature is depending on the material in which baking operation performed. Pickling operation is performed to remove scale and oxide product from the specimen and this is done by using acid. During the process acid breaks and causes for HE. To reduce these inhibitors are used during picking operation. These inhibitors have reduced the corrosion of material and simultaneously reduce the hydrogen entry in material [108].

Alloying

HE of materials is reduced by alloying some materials to the base materials such as aluminum, titanium. The alloying of aluminum to HSS creates a barrier for hydrogen diffusion because it can manipulate the binding energy and density of steel nearby the aluminum atom [110]. Titanium contents are also having a great influence on the mechanical properties of AHSS. These titanium particles converted into titanium carbide which has high binging energy and creates resistance for hydrogen diffusion [103]. It was found that if the material is having hydrogen concentration less the critical level of hydrogen concentration (Hc) then no failure occurs either on static or working condition [110–113].

HE prevention by plating

There is a wide variety of plating material and techniques available such as cadmium and nickel plating, titanium plating. Techniques that available are electroplating, mechanical plating, Ion plating (physical vapour deposition). By use of these appropriate plating, material susceptibility toward the HE was reduced as available in the literature [110,114–116]. Cadmium and nickel plating are used to reduce HE because they possess a low hydrogen diffusion coefficient. So, when AHSS materials are coated with cadmium then hydrogen entry inside the material reduced significantly. Zinc with nickel alloy plating was done to create a barrier for hydrogen diffusion. First nickel deposition was done because it had low hydrogen diffusion coefficient having a value of 5×10^{-11} m^2/s [117]. It was seen that some coating causes recombination of hydrogen atom taken place, form the hydrogen molecule and these molecules are escaped out before going inside the material. Cadmium possesses this quality of recombination of the hydrogen atom and reduces hydrogen entry [118]. Cadmium and titanium plating were introduced in the year of 1960 [120]. Cyaniding and non-cyaniding cadmium solutions were used with titanium compounds. Titanium percentage was very in cyaniding and non-cyaniding cadmium solution. It was found from an examination that a non-cyanide solution works more effectively and titanium compounds are more stable in it. This plating technique was used in coating threaded rods, shafts which working on high-stress environment, spring wire and structural steel having high strength [116,119]. Ion plating is also very effective for hydrogen diffusion barrier because this technique executes in a vacuum so that chances of hydrogen diffusion and embrittlement reduced considerably. Ion-plated Al coating has been utilized in craft application for quite twenty years [121].

Table 3 represents the various plating processes with corresponding hydrogen embrittlement index (EI) number. It was clearly understands from experimental results that zinc and nickel electroplated specimen have a least EI index. It was also seen that after baking treatment, EI was reduced considerably but incomplete recovery of coated specimen was occurs after baking treatment [115].

Prevention by coating

Wide variety of coating techniques are available such as vacuum deposited coating, chemical vapour deposition technique, organic coating, and electrophoretic deposition to deposit coated material such as graphene, niobium above the base material. Reduced graphene oxide layer reduces the hydrogen penetration during hydrogen charging. This was accomplished due to the formation of C–H bonds when cathodic charging was performed [29,104]. Bhadeshia explained that TiO_2, TiC, TiN, Cr_2O_3, alumina, BN and WC coating act as a barrier for hydrogen diffusion as shown in Fig. 12 [110]. These coatings reduce the hydrogen penetration rate inside the material considerably. Pt, Cu, Ag, Cd, Al and Au coatings also act as a resistance against HE [100]. Au and few Sn–Pb alloys coatings are terribly effective to reduce the permeation of hydrogen [122]. Pt coating having a layer thickness of 0.0015 μm can also reduce the hydrogen diffusion. The literature said that Cu is more efficient than Ni for the reduction of hydrogen diffusion in iron [123]. Alumina is very effective for prevention of material from HE. To deposit alumina over the steel, plasma coating technique was used and 1 μm thickness of crystal-like α-alumina deposited above the steel. In high temperature operating atmosphere such as 800 °C, this alumina coating is still adhered with the base material and work effectively. This alumina coating was reducing the tendency of hydrogen diffusion 3 to 4 times more as compared to base steel material [2,110,124]. The amorphous surface layer was very effective to prevent from HE. Phosphorus ion implantation technique was used for providing the amorphous layer above the base material. It has a disordered structure and creates a barrier for hydrogen penetration. Santos found that amorphous layer above iron base alloy has less hydrogen diffusion than the ferrite steel [125,126].

Prevention by diffusion layer

From literature, it was found that the carbon and nitrogen diffusion layer acts as a barrier for hydrogen entry to the base material and simultaneously reduces the crack propagation. If this diffusion layer has provided insufficient length, adhere to the base material and have a proper thickness with defect-free structure then HE chances are reduced [105]. Oxides surface layer causes hydrogen diffusion reduced to a certain extent

Table 3 – Plating process with corresponding hydrogen embrittlement index (EI).

SN	PLATING	EI
1	Cadmium plating	0.78
2	Zn plating	0.7
3	Zn–1%Co (pH 4.2) plating	0.63
4	Zn–Co–Fe plating	0.43
5	Zn–1%Co baked condition	0.11
6	Zn–10%Ni plating	0.037

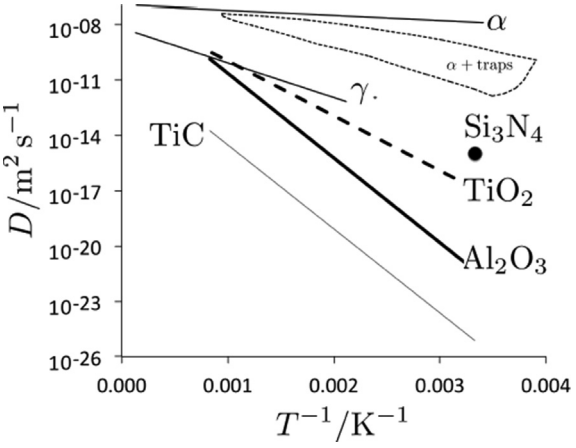

Fig. 12 – Represents the hydrogen diffusion coefficient of TiC, TiO_2, Al_2O_3, Si_3N_4 and compared with hydrogen diffusion coefficient of steel (α and γ stand for ferrite and austenite).

but not purely. The study also explained that the corrosion product reduces hydrogen penetration [100]. If stresses are acted in coated specimen then after some time these coating may damage and hydrogen can penetrate from coating to base material [127]. Elements which support the hydrogen entry to the base material are Te, Se, Sn, As, S, Hg, Pb, and Bi. These elements cause grain boundary separation to take place so avoided [100].

Trapped hydrogen

Hydrogen can be trapped in defects like dislocation, vacancy, grain boundaries and lattice irregularities [130]. This trapped hydrogen causes hydrogen-related failure (HE, hydrogen-induced cracking and hydrogen blistering) occur. Strong and sound trap causes HE susceptibility of steels are reduced. Trap having high activation energy can be considered as strong trap [183]. This trapping is categorized into two types, one is an irreversible trap and other is a reversible trap. In case of irreversible trapping, trapped hydrogen is not able to re-enter to the metal lattice and participate in diffusible hydrogen on the service life of steel while the reversible trap is able to re-enter in metal matrix and lattice. The difference between these traps was also categorized on the basis of trap or binding energy [128]. Table 4 shows the trapping sites with the corresponding activation energy for iron and steel. It is clearly shown in the table that hydrogen trapping sites such as in lattice, grain boundaries, dislocations, microvoids, and Fe oxide interface have low binding energy so these sites are represented as reversible trapping sites. Hydrogen trapping sites corresponding to high activation energy such as ferrite or cementite interface, non-metallic inclusion interface is called as irreversible trapping sites.

Thermal desorption experiment is used to distinguish between weak and irreversible trap hydrogen. It was said that weak trapped hydrogen is escaping out at low temperature whereas irreversibly trapped hydrogen is evolved at high temperature. It was also seen that actual de-trapping capacity of steel depends on the heating rate how much time has been provided to escape out all the trap hydrogen [110,129]. Thermal desorption spectroscopy (TDS) was used to calculate the trapping energy for all defects. This calculation was based on how these traps cause HE susceptibility can be reduced [132]. It was concluded that due to trapping, hydrogen solubility increases but diffusivity of hydrogen was reduced [130]. Saturated hydrogen content due to trapping is increased but this hydrogen is not harmful. These traps are responsible for delayed fracture mechanism of steel and it occurs when small stress relative to fracture strength acting for long service time and material failed in brittle nature [131]. Atomic traps cause hydrogen susceptibility of steel was reduced for examples such as on titanium-based Fe–Ti ferrite alloy and Al-added high Mn-TWIP steel [92,110,133]. Aluminum was responsible for changes in binding energy and density nearby Al atoms and thus Al-alloyed ferrite was more resistant for hydrogen than silicon added [134]. It was also concluded that ε-carbide have a good hydrogen trapping capability compared to cementite and this is possible because of with ferrite it has lower interfacial energy. Interfaces between Ferrite and cementite act like a weak trap but it causes hydrogen prompted cracking initiated. The binding energy of trap in interfaces between cementite-ferrite was 11–18 KJ/Mol and this trap was ineffective and useless [135,136]. Substitutionally alloyed carbides have a great tendency towards the hydrogen trap and reducing the HE effects. Vanadium centered carbides have a positive effect on reducing the hydrogen embrittlement and delayed failure of bolting steel and binding energy of that found to be 33 to 35 KJ/Mol [137]. So, it was concluded that binding energy (BE) plays an important role while studying hydrogen trap behavior. If BE is low then equilibrium exists between local trap hydrogen and lattice hydrogen. If hydrogen concentration in the matrix is reduced then these trap acts as hydrogen source and equilibrium was maintained. The trap would be more effective if it has high BE so that equilibrium diffusible hydrogen concentration in the matrix is much smaller than the concentration required for, HE.

Table 4 – Trapping sites with corresponding trapping activation energies in iron and steels.

S.N.	Trapping sites	Trapping activation energy (KJ/mol)
Reversible trapping sites		
1	Iron lattice	5.4–7.1
2	Grain boundary	17.2–18.6
3	Austenite/martensite interface	22
4	Dislocation	26.4–26.8
5	Austenite/dislocation boundary	37
6	Microvoid	35.2–40
7	Fe oxide interface	47
Irreversible trapping sites		
8	Ferrite/cementite interface	66.3–68.4
9	Cr carbide interface	67
10	Y2O3 interface	70
11	MnS interface	72
12	Al2O3 interface	79–86.2
13	Fe3C interface	84
14	TiC interface	68–137

Conclusion

The effect on hydrogen in mechanical properties of AHSS material was seen by a wide variety of examination techniques such as LIST and SSRT and it was found that mechanical properties (strength and ductility) are get decreased. Fractographic and microstructure examination of the fractured material was done and it was clearly indicated that the HE effects on the final fracture of the material. Some key points are discussed below.

I. DP steels are highly susceptible to hydrogen-related failure widely known as HE. Due to the effect of hydrogen, mechanical properties of DP steels are getting reduced and microstructure is changed. Fractography examination is also suggested that the final fracture of the material was taken place in brittle (transgranular) in nature.
II. TRIP steels are also affected due to the effect of HE. During the transformation period, austenite converted

into martensite and excess hydrogen gets released. If this excess hydrogen accumulates at the crack tip than the crack growth will take place after some time due to the effect of the accumulated hydrogen and ductility of material is reduced. During fractography examination, it was found that cracks were initiated from martensite islands and propagated towards the soft ferrite region. A similar observation was seen during the investigation of CP steels.

III. The effect of hydrogen in TWIP steels is still unclear. Some authors suggested that no effect of hydrogen in mechanical as well as microstructure of TWIP steel and some found the considerable degradation in mechanical properties. The brittle transgranular fracture was seen in the fractographic examination due to the effect of hydrogen in TWIP steels. If the martensitic structure is enclosed by the reserved austenite then due to austenite behaves as a sink for the hydrogen atom, hydrogen embrittlement susceptibility will get reduced and they provide more resistant for hydrogen diffusion.

IV. Hydrogen trap capacity of retained austenite is quite high with high binding energy. Ones the hydrogen gets trapped in austenite; it is difficult for a hydrogen atom to come out because they produce strong trap with high binding energy. If ferrite is surrounded by the austenite then hydrogen mobility will be reduced through the AHSS structure and HE susceptibility reduces.

V. Prevention activities from HE were discussed in detail such as applying a coating of graphene and niobium, cadmium and nickel electroplating, alloying of Al to AHSS material and providing carbon and nitrogen diffusion layer. By applying these preventing methods, hydrogen diffusion in material and influence in mechanical properties of AHSS material are reduced significantly.

VI. The effect of hydrogen in AHSS materials was determined experimentally in laboratory working condition. But when the material is working in actual operating condition or environment, it will behave differently because the actual operating condition (temperature, working stress, moisture) will differ from the controlled laboratory condition. So, to how much extent actual result correlates with the experimental one is still unclear.

Further work will be carried out to simulate the experimental work with actual working condition. Still, the right mechanism by which this degradation phenomenon (HE) has taken place is unclear. Future research will be done on the selection of suitable coating to reduce the hydrogen embrittlement susceptibility of AHSS material.

REFERENCES

[1] Liu Q, Zhou Q, Venezuela J, Zhang M, Wang J, Atrens A. A review of the influence of hydrogen on the mechanical properties of DP, TRIP, and TWIP advanced high-strength steels for auto construction. Corros Rev 2016 Jun 1;34(3):127–52.

[2] Dwivedi SK, Vishwakarma M. Hydrogen embrittlement in different materials: a review. Int J Hydrogen Energy 2018;43(46):21603–16.

[3] Atrens A, Liu Q, Tapia-Bastidas C, Gray E, Irwanto B, Venezuela J, Liu Q. Influence of hydrogen on steel components for clean energy. Corrosion and Materials Degradation 2018 Dec;1(1):3–26.

[4] Liu Q, Atrens A. Reversible hydrogen trapping in a 3.5 NiCrMoV medium strength steel. Corros Sci 2015 Jul 1;96:112–20.

[5] Liu Q, Irwanto B, Atrens A. Influence of hydrogen on the mechanical properties of some medium-strength Ni–Cr–Mo steels. Mater Sci Eng A 2014 Nov 3;617:200–10.

[6] Venezuela J, Blanch J, Zulkiply A, Liu Q, Zhou Q, Zhang M, Atrens A. Further study of the hydrogen embrittlement of martensitic advanced high-strength steel in simulated auto service conditions. Corros Sci 2018 May 1;135:120–35.

[7] Gangloff RP. Hydrogen assisted cracking of high strength alloys. Aluminum Co of America Alcoa Center PA Alcoa Technical Center; 2003 Aug.

[8] Lynch SP. Hydrogen embrittlement (HE) phenomena and mechanisms. In: Stress corrosion cracking; 2011. p. 90–130.

[9] Louthan MR. Hydrogen embrittlement of metals: a primer for the failure analyst. J Fail Anal Prev 2008 Jun 1;8(3):289–307.

[10] Depover T, Escobar DP, Wallaert E, Zermout Z, Verbeken K. Effect of hydrogen charging on the mechanical properties of advanced high strength steels. Int J Hydrogen Energy 2014 Mar 18;39(9):4647–56.

[11] Hilditch T, Lee S, Speer J, Matlock D. Response to Hydrogen Charging in High Strength Automotive Sheet Steel Products. 2003. https://doi.org/10.4271/2003-01-0525. SAE Technical Paper 2003-01-0525.

[12] Becker WT. Ductile and brittle fracture 2002.

[13] Lynch SP. Metallographic and fractographic techniques for characterising and understanding hydrogen-assisted cracking of metals. In: Gaseous hydrogen embrittlement of materials in energy technologies: the problem, its characterisation and effects on particular alloy classes; 2012. p. 274–346.

[14] Gangloff RP, Somerday BP, editors. Gaseous hydrogen embrittlement of materials in energy technologies: mechanisms, modelling and future developments. Elsevier; 2012 Jan 19.

[15] Song J, Curtin WA. Atomic mechanism and prediction of hydrogen embrittlement in iron. Nat Mater 2013 Feb;12(2):145.

[16] Dwivedi SK, Vishwakarma M, Ahmed S. Experimental investigation of hydrogen embrittlement during coating process and effect on mechanical properties of high strength steel used for fasteners. Mater Today: Proceedings 2018 Jan 1;5(9):18707–15.

[17] McMahon Jr CJ. Hydrogen-induced intergranular fracture of steels. Eng Fract Mech 2001 Apr 1;68(6):773–88.

[18] Venezuela J, Liu Q, Zhang M, Zhou Q, Atrens A. The influence of hydrogen on the mechanical and fracture properties of some martensitic advanced high strength steels studied using the linearly increasing stress test. Corros Sci 2015 Oct 1;99:98–117.

[19] Lynch SP. Hydrogen embrittlement phenomena and mechanisms. Corros Rev 2012a;30:105–23.

[20] Moli-Sanchez L, Martin F, Leunis E, Briottet L, Lemoine P, Chene J. Comparison of the tensile behavior of a tempered 34CrMo4 steel exposed in situ to high pressure H2 gas or to cathodic H charging. In: SteelyHydrogen2014 conference proceedings; 2014. p. 448–61.

[21] Ramamurthy S, Atrens A. Stress corrosion cracking of high strength steels. Corros Rev 2013 Mar 1;31(1):1–31.
[22] Venezuela J, Zhou Q, Liu Q, Zhang M, Atrens A. Hydrogen trapping in some automotive martensitic advanced highstrength steels. Adv Eng Mater 2018 Jan;20(1):1700468.
[23] Atrens A, Liu Q, Zhou Q, Venezuela J, Zhang M. Evaluation of automobile service performance using laboratory testing. Mater Sci Technol 2018 Jul 14:1–7.
[24] Venezuela J, Zhou Q, Liu Q, Li H, Zhang M, Dargusch MS, et al. The inflence of microstructure on the hydrogen embrittlement susceptibility of martensitic advanced high strength steels. Mater Today Commun 2018 Dec 1;17:1–4.
[25] Liu Q, Zhou Q, Venezuela J, Zhang M, Atrens A. Evaluation of the influence of hydrogen on some commercial DP, Q&P and TWIP advanced high-strength steels during automobile service. Eng Fail Anal 2018 Dec 1;94:249–73.
[26] Venezuela J, Liu Q, Zhang M, Zhou Q, Atrens A. A review of hydrogen embrittlement of martensitic advanced high-strength steels. Corros Rev 2016 Jun 1;34(3):153–86.
[27] Demeri MY. Advanced high-strength steels: science, technology, and applications. ASM international; 2013 Aug 1.
[28] Saini N, Pandey C, Mahapatra MM. Effect of diffusible hydrogen content on embrittlement of P92 steel. Int J Hydrogen Energy 2017 Jul 6;42(27):17328–38.
[29] Kim YS, Kim JG. Electroplating of reduced-graphene oxide on austenitic stainless steel to prevent hydrogen embrittlement. Int J Hydrogen Energy 2017 Nov 2;42(44):27428–37.
[30] Wang M, Akiyama E, Tsuzaki K. Effect of hydrogen on the fracture behavior of high strength steel during slow strain rate test. Corros Sci 2007 Nov 1;49(11):4081–97.
[31] Escobar DP, Verbeken K, Duprez L, Verhaege M. Evaluation of hydrogen trapping in high strength steels by thermal desorption spectroscopy. Mater Sci Eng A 2012 Aug 15;551:50–8.
[32] Verbeken K. Analysing hydrogen in metals: bulk thermal desorption spectroscopy (TDS) methods. In: Gaseous hydrogen embrittlement of materials in energy technologies: mechanisms, modelling and future developments; 2012. p. 27–55.
[33] Williams DB, Carter CB. Transmission electron microscopy: a textbook for materials science. 2009.
[34] Mertens G, Duprez L, De Cooman BC, Verhaege M. Hydrogen absorption and desorption in steel by electrolytic charging. In: Advanced Materials Research, vol. 15; 2007. p. 816–21 [Trans Tech Publications].
[35] Danford MD. Hydrogen trapping and the interaction of hydrogen with metals. NASA Technical Paper 2744. 1987.
[36] Venezuela J, Zhou Q, Liu Q, Zhang M, Atrens A. Influence of hydrogen on the mechanical and fracture properties of some martensitic advanced high strength steels in simulated service conditions. Corros Sci 2016 Oct 1;111:602–24.
[37] Daw MS, Baskes MI, Bisson CL, Wolfer WG, Jones RH, Gerberich WW. Modeling environmental effects on crack growth processes. New York: TMS-AIME; 1986.
[38] Bouaziz O, Zurob H, Huang M. Driving force and logic of development of advanced high strength steels for automotive applications. Steel Res Int 2013 Oct;84(10):937–47.
[39] Matlock DK, Speer JG, De Moor E, Gibbs PJ. Recent developments in advanced high strength sheet steels for automotive applications: an overview. Jestech 2012 Apr 2;15(1):1–2.
[40] Galán J, Samek L, Verleysen P, Verbeken K, Houbaert Y. Advanced high strength steels for automotive industry. Rev Metal (Madr) 2012 Jan 1;48(2):118–31.
[41] Tamarelli CM. Ahss 101: the evolving use of advanced high strength steels for automotive applications. 2011.
[42] Granbom Y. Structure and mechanical properties of dual phase steels: an experimental and theoretical analysis. Doctoral dissertation. KTH; 2010.
[43] MI K, Biro E, Zhou Y. Microstructure and mechanical properties of resistance spot welded advanced high strength steels. Mater Trans 2008 Jul 1;49(7):1629–37.
[44] Speer JG, De Moor E, Findley KO, Matlock DK, De Cooman BC, Edmonds DV. Analysis of microstructure evolution in quenching and partitioning automotive sheet steel. Metall Mater Trans A 2011 Dec 1;42(12):3591.
[45] Edmonds DV, He K, Rizzo FC, De Cooman BC, Matlock DK, Speer JG. Quenching and partitioning martensite—a novel steel heat treatment. Mater Sci Eng A 2006 Nov 25;438:25–34.
[46] ULSAB-AVC Consortium. reportULSAB-AVC (advanced vehicle concepts) overview report.
[47] Liu H, Li F, Shi W, Swaminathan S, He Y, Rohwerder M, Li L. Challenges in hot-dip galvanizing of high strength dual phase steel: surface selective oxidation and mechanical property degradation. Surf Coat Technol 2012 Apr 15;206(16):3428–36.
[48] Oliver S, Jones TB, Fourlaris G. Dual phase versus TRIP strip steels: microstructural changes as a consequence of quasi-static and dynamic tensile testing. Mater Char 2007 Apr 1;58(4):390–400.
[49] Keeler S, Kimchi M. Advanced high-strength steels application guidelines V5. WorldAutoSteel; 2015 Apr 28.
[50] Huang J, Poole WJ, Militzer M. Austenite formation during intercritical annealing. Metall Mater Trans A 2004 Nov 1;35(11):3363–75.
[51] Jiang HT, Tang D, Mi ZL. Latest progress in development and application of advanced high strength steels for automobiles. Gangtie Yanjiu Xuebao 2007;19(8):1–6.
[52] Chen L, Zhao Y, Qin X. Some aspects of high manganese twinning-induced plasticity (TWIP) steel, a review. Acta Metall Sin 2013 Feb 1;26(1):1–5.
[53] Neu RW. Performance and characterization of TWIP steels for automotive applications. Materials Performance and Characterization 2013 Aug 23;2(1):244–84.
[54] Ferraiuolo A, Smith A, Sevillano JG, De Las Cuevas F, Karjalainen P, Pratolongo G, Gouveia H, Rodrigues MM. Metallurgical design of high strength austenitic Fe-C-Mn steels with excellent formability (metaldesign). Luxembourg: European Union; 2012. p. 162.
[55] Chung K, Ma N, Park T, Kim D, Yoo D, Kim C. A modified damage model for advanced high strength steel sheets. Int J Plast 2011 Oct 1;27(10):1485–511.
[56] De Cooman BC, Chen L, Kim HS, Estrin Y, Kim SK, Voswinckel H. State-of-the-science of high manganese TWIP steels for automotive applications. In: Microstructure and texture in steels. London: Springer; 2009. p. 165–83.
[57] De Cooman BC, Kwon O, Chin KG. State-of-the-knowledge on TWIP steel. Mater Sci Technol 2012 May 1;28(5):513–27.
[58] Park IJ, Jeong KH, Jung JG, Lee CS, Lee YK. The mechanism of enhanced resistance to the hydrogen delayed fracture in Al-added Fe–18Mn–0.6 C twinning-induced plasticity steels. Int J Hydrogen Energy 2012 Jun 1;37(12):9925–32.
[59] Cornette D, Hourman T, Hudin O, Laurent JP, Reynaert A. High strength steels for automotive safety parts. SAE Technical Paper; 2001 Mar 5.
[60] Kuziak R, Kawalla R, Waengler S. Advanced high strength steels for automotive industry. Archives of Civil and Mechanical Engineering 2008 Jan 1;8(2):103–17.
[61] Koyama M, Akiyama E, Tsuzaki K. Hydrogen embrittlement in a Fe–Mn–C ternary twinning-induced plasticity steel. Corros Sci 2012 Jan 1;54:1–4.

[62] Winzer N, Atrens A, Dietzel W, Song G, Kainer KU. Comparison of the linearly increasing stress test and the constant extension rate test in the evaluation of transgranular stress corrosion cracking of magnesium. Mater Sci Eng A 2008 Jan 15;472(1–2):97–106.
[63] Koyama M, Akiyama E, Sawaguchi T, Raabe D, Tsuzaki K. Hydrogen-induced cracking at grain and twin boundaries in an Fe–Mn–C austenitic steel. Scr Mater 2012 Apr 1;66(7):459–62.
[64] Villalba E, Atrens A. Hydrogen embrittlement and rock bolt stress corrosion cracking. Eng Fail Anal 2009 Jan 1;16(1):164–75.
[65] Lovicu G, Bottazzi M, D'Aiuto F, De Sanctis M, Dimatteo A, Santus C, Valentini R. Hydrogen embrittlement of automotive advanced high-strength steels. Metall Mater Trans A 2012 Nov 1;43(11):4075–87.
[66] Villalba E, Atrens A. Metallurgical aspects of rock bolt stress corrosion cracking. Mater Sci Eng A 2008 Sep 15;491(1–2):8–18.
[67] Ryu JH, Chun YS, Lee CS, Bhadeshia HK, Suh DW. Effect of deformation on hydrogen trapping and effusion in TRIP-assisted steel. Acta Mater 2012 Jun 1;60(10):4085–92.
[68] Begić Hadžipašić A, Malina J, Malina M. The influence of microstructure on hydrogen diffusion and embrittlement of multiphase fine-grained steels with increased plasticity and strength. Chem Biochem Eng Q 2011 Jun 30;25(2):159–69.
[69] So KH, Kim JS, Chun YS, Park KT, Lee YK, Lee CS. Hydrogen delayed fracture properties and internal hydrogen behavior of a Fe-18Mn-1.5Al-0.6C TWIP steel. ISIJ Int 2009;49:1952–9.
[70] Zhu X, Li W, Zhao H, Wang L, Jin X. Hydrogen trapping sites and hydrogen-induced cracking in high strength quenching & partitioning (Q&P) treated steel. Int J Hydrogen Energy 2014 Aug 13;39(24):13031–40.
[71] Takashima K, Yoshioka Y, Yokoyama KI, Funakawa Y. Hydrogen embrittlement behavior of ultra-high strength dual phase steel sheet under sustained tensile-loading test. ISIJ Int 2018 Jan 15;58(1):173–8.
[72] Liu Q, Irwanto B, Atrens A. The influence of hydrogen on 3.5 NiCrMoV steel studied using the linearly increasing stress test. Corros Sci 2013 Feb 1;67:193–203.
[73] Loidl M, Kolk O, Veith S, Göbel T. Characterization of hydrogen embrittlement in automotive advanced high strength steels. Mater Werkst 2011 Dec;42(12):1105–10.
[74] Davies RG. Hydrogen embrittlement of dual-phase steels. Metallurgical Transactions A 1981 Sep 1;12(9):1667–72.
[75] Sun S, Gu J, Chen N. The influence of hydrogen on the sub-structure of the martensite and ferrite dual-phase steel. Scr Metall 1989 Oct 1;23(10):1735–7.
[76] Depover T, Wallaert E, Verbeken K. Fractographic analysis of the role of hydrogen diffusion on the hydrogen embrittlement susceptibility of DP steel. Mater Sci Eng A 2016 Jan 1;649:201–8.
[77] Hirth JP. Effects of hydrogen on the properties of iron and steel. Metallurgical Transactions A 1980 Jun 1;11(6):861–90.
[78] Mine Y, Horita Z, Murakami Y. Effect of hydrogen on martensite formation in austenitic stainless steels in high-pressure torsion. Acta Mater 2009 Jun 1;57(10):2993–3002.
[79] Ronevich JA, Speer JG, Matlock DK. Hydrogen embrittlement of commercially produced advanced high strength sheet steels. SAE Int J Mater Manufac 2010 Jan 1;3(1):255–67.
[80] Sojka J, Vodárek V, Schindler I, Ly C, Jérôme M, Váňová P, Ruscassier N, Wenglorzová A. Effect of hydrogen on the properties and fracture characteristics of TRIP 800 steels. Corros Sci 2011 Aug 1;53(8):2575–81.
[81] Imlau J, Bleck W, Zaefferer S. Comparison of damage development depending on the local microstructure in low alloyed Al-TRIP-steels, IF steel and a DP steel. Int J Mater Res 2009;100(4):584–93.
[82] Laureys A, Depover T, Petrov R, Verbeken K. Microstructural characterization of hydrogen induced cracking in TRIP-assisted steel by EBSD. Mater Char 2016 Feb 1;112:169–79.
[83] Zhu X, Li W, Zhao H, Jin X. Effects of cryogenic and tempered treatment on the hydrogen embrittlement susceptibility of TRIP-780 steels. Int J Hydrogen Energy 2013 Aug 21;38(25):10694–703.
[84] Escobar DP, Miñambres C, Duprez L, Verbeken K, Verhaege M. Internal and surface damage of multiphase steels and pure iron after electrochemical hydrogen charging. Corros Sci 2011 Oct 1;53(10):3166–76.
[85] McCoy RA. Development of a high-strength manganese steel resistant to hydrogen embrittlement. InProceedings of the International Conference on the Effects of Hydrogen on Materials Properties and Selection and Structural Design. ASM; 1973. p. 169–78.
[86] Ronevich JA, De Cooman BC, Speer JG, De Moor E, Matlock DK. Hydrogen effects in prestrained transformation induced plasticity steel. Metall Mater Trans A 2012 Jul 1;43(7):2293–301.
[87] Hojo T, Kobayashi J, Kajiyama T, Sugimoto KI, Count A. Effects of alloying elements on impact properties of ultra high-strength TRIP-aided bainitic ferrite steels. Jn Shān Gāo Zhuān Jì Yào. 2010;(52):9–16.
[88] Jung JK, Lee OY, Park YK, Kim DE, Jin KG. Hydrogen embrittlement behavior of high Mn TRIP/TWIP steels. Korean J Mater Res 2008;18(7):394–9.
[89] Ronevich JA, Kim SK, Speer JG, Matlock DK. Hydrogen effects on cathodically charged twinning-induced plasticity steel. Scr Mater 2012 Jun 1;66(12):956–9.
[90] Chin KG, Kang CY, Shin SY, Hong S, Lee S, Kim HS, Kim KH, Kim NJ. Effects of Al addition on deformation and fracture mechanisms in two high manganese TWIP steels. Mater Sci and Eng A 2011 Mar 15;528(6):2922–8.
[91] Chun YS, Park KT, Lee CS. Delayed static failure of twinning-induced plasticity steels. Scr Mater 2012 Jun 1;66(12):960–5.
[92] Suh DW. Critical assessment 2: hydrogen induced fracture in austenitic, high-manganese TWIP steel. Mater Sci Technol 2014 Aug 1;30(10):1131–4.
[93] Koyama M, Akiyama E, Tsuzaki K. Effect of hydrogen content on the embrittlement in a Fe–Mn–C twinning-induced plasticity steel. Corros Sci 2012 Jun 1;59:277–81.
[94] Allain S, Chateau JP, Bouaziz O, Migot S, Guelton N. Correlations between the calculated stacking fault energy and the plasticity mechanisms in Fe–Mn–C alloys. Mater Sci and Eng A 2004 Dec 15;387:158–62.
[95] Lee YK. Microstructural evolution during plastic deformation of twinning-induced plasticity steels. Scr Mater 2012 Jun 1;66(12):1002–6.
[96] Curtze S, Kuokkala VT. Dependence of tensile deformation behavior of TWIP steels on stacking fault energy, temperature and strain rate. Acta Mater 2010 Sep 1;58(15):5129–41.
[97] Yang Q, Luo JL. Martensite transformation and surface cracking of hydrogen charged and outgassed type 304 stainless steel. Mater Sci and Eng A 2000 Aug 31;288(1):75–83.
[98] Pontini AE, Hermida JD. X-ray diffraction measurement of the stacking fault energy reduction induced by hydrogen in an AISI 304 steel. Scr Mater 1997 Dec 1;37(11).
[99] Ryu JH, Kim SK, Lee CS, Suh DW, Bhadeshia HK. Effect of aluminium on hydrogen-induced fracture behaviour in austenitic Fe–Mn–C steel. Proc R Soc A Math Phys Eng Sci 2013 Jan 8;469(2149):20120458.
[100] Ćwiek J. Prevention methods against hydrogen degradation of steel. Journal of Achievements in Materials and Manufacturing Engineering 2010 Nov;43(1):214–21.

[101] Timmins PF. Solutions to hydrogen attack in steels.
[102] Grobin Jr AW. Other ASTM committees and ISO committees involved in hydrogen embrittlement test methods. Hydrogen Embrittlement: Prev Control 1988 Jan;962:46.
[103] Kim HJ, Jeon SH, Yang WS, Yoo BG, Chung YD, Ha HY, Chung HY. Effects of titanium content on hydrogen embrittlement susceptibility of hot-stamped boron steels. J Alloy Comp 2018 Feb 25;735:2067–80.
[104] Nam TH, Lee JH, Choi SR, Yoo JB, Kim JG. Graphene coating as a protective barrier against hydrogen embrittlement. Int J Hydrogen Energy 2014 Jul 24;39(22):11810–7.
[105] Michler T, Naumann J. Coatings to reduce hydrogen environment embrittlement of 304 austenitic stainless steel. Surf Coat Technol 2009 Mar 25;203(13):1819–28.
[106] De Souza Brandolt C, Noronha LC, Hidalgo GE, Takimi AS, Schroeder RM, de Fraga Malfatti C. Niobium coating applied by HVOF as protection against hydrogen embrittlement of API 5CT P110 steel. Surf Coat Technol 2017 Aug 15;322:10–8.
[107] https://www.worldautosteel.org/why-steel/fuel-efficiency.
[108] Figueroa D, Robinson MJ. The effects of sacrificial coatings on hydrogen embrittlement and re-embrittlement of ultra high strength steels. Corros Sci 2008 Apr 1;50(4):1066–79.
[109] https://en.wikipedia.org/wiki/Hydrogen_embrittlement.
[110] Bhadeshia HK. Prevention of hydrogen embrittlement in steels. ISIJ Int 2016 Jan 15;56(1):24–36.
[111] Yamasaki S, Takahashi T. Evaluation method of delayed fracture property of high strength steels. Tetsu-To-Hagane 1997 Jul 1;83(7):454–9.
[112] Tarui T, Yamasaki S. Evaluation method of delayed fracture property and overcoming techniques of delayed fracture of high strength steels. Tetsu-To-Hagane 2002;88(10):612–9.
[113] Suzuki N, Ishii N, Miyagawa T, Harada H. Estimation of delayed fracture property of steels. Tetsu-To-Hagane 1993 Feb 1;79(2):227–32.
[114] Nascimento MP, Souza RC, Pigatin WL, Voorwald HJ. Effects of surface treatments on the fatigue strength of AISI 4340 aeronautical steel. Int J Fatigue 2001 Aug 1;23(7):607–18.
[115] Hillier EM, Robinson MJ. Hydrogen embrittlement of high strength steel electroplated with zinc–cobalt alloys. Corros Sci 2004 Mar 1;46(3):715–27.
[116] Durney LJ, editor. Graham's electroplating engineering handbook. Springer Science & Business Media; 1984 Nov 30.
[117] Hill ML, Johnson EW. The diffusivity of hydrogen in nickel. Acta Metall 1955 Nov 1;3(6):566–71.
[118] Kim H, Popov BN, Chen KS. Comparison of corrosion-resistance and hydrogen permeation properties of Zn–Ni, Zn–Ni–Cd and Cd coatings on low-carbon steel. Corros Sci 2003 Jul 1;45(7):1505–21.
[119] Wang SS, Chai JK, Shui YM, Liang JK. Cd–Ti electrodeposits from a noncyanide bath. Plat Surf Finish 1981 Dec;68(12):62–4.
[120] Takata K. Japanese patents SHO-35 18260 (1960) and SHO-38 20703. 1963.
[121] Fannin ER, Muehlberger DE. Ivadizer applied aluminum coating improves corrosion protection of aircraft. McDonnell Aircraft Company; 1978. p. 26.
[122] Perng TP, Johnson MJ, Altstetter CJ. Hydrogen permeation through coated and uncoated WASPALOY. Metallurgical Transactions A 1988 May 1;19(5):1187–92.
[123] Chatterjee SS, Ateya BG, Pickering HW. Effect of electrodeposited metals on the permeation of hydrogen through iron membranes. Metallurgical transactions A 1978 Mar 1;9(3):389–95.
[124] Levchuk D, Koch F, Maier H, Bolt H. Deuterium permeation through eurofer and α-alumina coated eurofer. J Nucl Mater 2004 Jul 1;328(2–3):103–6.
[125] Ensinger W, Wolf GK. Protection against hydrogen embrittlement by ion beam mixing. Nucl Instrum Methods Phys Res Sect B Beam Interact Mater Atoms 1989 Mar 2;39(1–4):552–5.
[126] Dos Santos DS, De Miranda PV. J Mater Sci 1997;32:6311–5.
[127] Hollenberg GW, Simonen EP, Kalinin G, Terlain A. Tritium/hydrogen barrier development. Fusion Eng Des 1995 Mar 2;28:190–208.
[128] Michler T, Balogh MP. Hydrogen environment embrittlement of an ODS RAF steel–Role of irreversible hydrogen trap sites. Int J Hydrogen Energy 2010 Sep 1;35(18):9746–54.
[129] Katano G, Ueyama K, Mori M. Observation of hydrogen distribution in high-strength steel. J Mater Sci 2001 May 1;36(9):2277–86.
[130] Krom AH, Bakker AD. Hydrogen trapping models in steel. Metall Mater Trans B 2000 Dec 1;31(6):1475–82.
[131] Frohmberg RP, Barnett WJ, Troiano AR. Delayed failure and hydrogen embrittlement in steel. Case Inst of Tech Cleveland OH; 1954 Jun.
[132] Serra E, Perujo A, Benamati G. Influence of traps on the deuterium behaviour in the low activation martensitic steels F82H and Batman. J Nucl Mater 1997 Jun 1;245(2–3):108–14.
[133] Kim HJ, Youn SK. Three dimensional analysis of high frequency induction welding of steel pipes with impeder. J Manuf Sci Eng 2008 Jun 1;130(3). 031005.
[134] Li Y, Chen C, Zhang F. Al and Si influences on hydrogen embrittlement of carbide-free bainitic steel. Adv Mater Sci Eng 2013;2013.
[135] Choo WY, Lee JY. Thermal analysis of trapped hydrogen in pure iron. Metallurgical Transactions A 1982 Jan 1;13(1):135–40.
[136] Hong GW, Lee JY. The interaction of hydrogen and the cementite-ferrite interface in carbon steel. J Mater Sci 1983 Jan 1;18(1):271–7.
[137] Kawakami K, Matsumiya T. Numerical analysis of hydrogen trap state by TiC and V4C3 in bcc-Fe. ISIJ Int 2012;52(9):1693–7.
[138] Lynch SP. Mechanisms of hydrogen assisted cracking–a review. Hydrogen effects on material behaviour and corrosion deformation interactions. 2003. p. 449–66.
[139] Zaferani SH, Miresmaeili R, Pourcharmi MK. Mechanistic models for environmentally-assisted cracking in sour service. Eng Fail Anal 2017 Sep 1;79:672–703.
[140] Kappes M, Iannuzzi M, Carranza RM. Hydrogen embrittlement of magnesium and magnesium alloys: a review. J Electrochem Soc 2013 Jan 1;160(4):C168–78.
[141] Lu G, Zhang Q, Kioussis N, Kaxiras E. Hydrogen-enhanced local plasticity in aluminum: an ab initio study. Phys Rev Lett 2001 Aug 8;87(9). 095501.
[142] Robertson IM. The effect of hydrogen on dislocation dynamics. Eng Fract Mech 1999 Nov 1;64(5):649–73.
[143] Liang Y, Ahn DC, Sofronis P, Dodds Jr RH, Bammann D. Effect of hydrogen trapping on void growth and coalescence in metals and alloys. Mech Mater 2008 Mar 1;40(3):115–32.
[144] Pundt A, Kirchheim R. Hydrogen in metals: microstructural aspects. Annu Rev Mater Res 2006 Aug 4;36:555–608.
[145] Nibur KA, Bahr DF, Somerday BP. Hydrogen effects on dislocation activity in austenitic stainless steel. Acta Mater 2006 Jun 1;54(10):2677–84.
[146] Atrens A, Venezuela J, Liu Q, Zhou Q, Verbeken K, Tapia-Bastidas C, Gray E, Christien F, Wolski K. Electrochemical and mechanical aspects of hydrogen embrittlement evaluation of martensitic steels. 2018. p. 201–25.
[147] Eliaz N, Shachar A, Tal B, Eliezer D. Characteristics of hydrogen embrittlement, stress corrosion cracking and tempered martensite embrittlement in high-strength steels. Eng Fail Anal 2002 Apr 1;9(2):167–84.

[148] Venezuela J, Zhou Q, Liu Q, Zhang M, Atrens A. Hydrogen trapping in some automotive martensitic advanced high-strength steels. Adv Eng Mater 2018 Jan;20(1):1700468.
[149] Venezuela JJ. The influence of hydrogen on MS980, MS1180, MS1300 and MS1500 martensitic advanced high strength steels used for automotive applications. 2017.
[150] Pradhan PK, Robi PS, Roy SK. Micro void coalescence of ductile fracture in mild steel during tensile straining. Frat Ed Integrità Strutt 2012;6(19).
[151] Lynch S. Discussion of some recent literature on hydrogen-embrittlement mechanisms: addressing common misunderstandings. Corros Rev 2019;37(5):377–95.
[152] Lynch SP. Metallographic contributions to understanding mechanisms of environmentally assisted cracking. Metallography 1989 Sep 1;23(2):147–71.
[153] Salleh MM, Al Bakri AM, Abdullah A, Kamarudin H. Failure modes of hydrogen damage on metal tubes. Australian Journal of Basic and Applied Sciences 2013;7(5):329–35.
[154] Kilic Suleyman And Ozturk Fahrettin; Recent trends of application of advanced high-strength steels in automotive industry to enhance sustainability; The 16th International Conference On Machine Design And Production June 30 – July 03 2014, [İzmir, Türkiye].
[155] www.worldautosteel.org.
[156] Kagay BJ. Hydrogen embrittlement testing of alloy 718 for oil and gas applications. Doctoral dissertation. Colorado School of Mines. Arthur Lakes Library; 2016.
[157] Djukic MB, Zeravcic VS, Bakic GM, Sedmak A, Rajicic B. Hydrogen damage of steels: a case study and hydrogen embrittlement model. Eng Fail Anal 2015 Dec 1;58:485–98.
[158] Luo H, Li Z, Raabe D. Hydrogen enhances strength and ductility of an equiatomic high-entropy alloy. Sci Rep 2017 Aug 29;7(1):9892.
[159] Cheaitani MJ, Pargeter RJ. Fracture mechanics techniques for assessing the effects of hydrogen on steel properties. In: International Steel and Hydrogen Conference; 2011 Sep. p. 1–7.
[160] Djukic MB, Bakic GM, Zeravcic VS, Sedmak A, Rajicic B. The synergistic action and interplay of hydrogen embrittlement mechanisms in steels and iron: localized plasticity and decohesion. Eng Fract Mech 2019 Jun 28:106528.
[161] Koyama M, Tasan CC, Akiyama E, Tsuzaki K, Raabe D. Hydrogen-assisted decohesion and localized plasticity in dual-phase steel. Acta Mater 2014;70:174–87.
[162] Snir Y, Haroush S, Danon A, Landau A, Gelbstein Y, Eliezer D. Metallurgical and hydrogen effects on the small punch tested mechanical properties of PH-13-8Mo stainless steel. Materials 2018;11(10):1966.
[163] Kumar S, Namboodhiri TK. Precipitation hardening and hydrogen embrittlement of aluminum alloy AA7020. Bull Mater Sci 2011 Apr 1;34(2):311–21.
[164] Omura T, Nakamura J. Hydrogen embrittlement properties of stainless and low alloy steels in High pressure gaseous hydrogen environment. ISIJ Int 2012;52(2):234–9.
[165] Symons DM. A comparison of internal hydrogen embrittlement and hydrogen environment embrittlement of X-750. Eng Fract Mech 2001 Apr 1;68(6):751–71.
[166] Komazaki SI, Koyama A, Misawa T. Effect of morphology of copper precipitation particles on hydrogen embrittlement behavior in Cu-added ultra low carbon steel. Mater Trans 2002;43(9):2213–8.
[167] Symons DM. Hydrogen embrittlement of Ni-Cr-Fe alloys. Metall Mater Trans A 1997 Mar 1;28(3):655–63.
[168] Depover T, Van den Eeckhout E, Verbeken K. The impact of hydrogen on the ductility loss of bainitic Fe–C alloys. Mater Sci Technol 2016 Oct 12;32(15):1625–31.
[169] Depover T, Laureys A, Pérez Escobar D, Van den Eeckhout E, Wallaert E, Verbeken K. Understanding the interaction between a steel microstructure and hydrogen. Materials 2018 May;11(5):698.
[170] Guan K, Szpunar JA, Matocha K, Wang D. Study on temper embrittlement and hydrogen embrittlement of a hydrogenation reactor by small punch test. Materials 2017;10(6):671.
[171] Gholami T, Salavati-Niasari M, Varshoy S. Investigation of the electrochemical hydrogen storage and photocatalytic properties of CoAl2O4 pigment: green synthesis and characterization. Int J Hydrogen Energy 2016 Jun 15;41(22):9418–26.
[172] Gholami T, Salavati-Niasari M. Effects of copper: aluminum ratio in CuO/Al2O3 nanocomposite: electrochemical hydrogen storage capacity, band gap and morphology. Int J Hydrogen Energy 2016 Sep 14;41(34):15141–8.
[173] Endo N, Suzuki S, Goshome K, Maeda T. Operation of a bench-scale TiFe-based alloy tank under mild conditions for low-cost stationary hydrogen storage. Int J Hydrogen Energy 2017 Feb 23;42(8):5246–51.
[174] Sangsefidi FS, Salavati-Niasari M, Khojasteh H, Shabani-Nooshabadi M. Synthesis, characterization and investigation of the electrochemical hydrogen storage properties of CuO–CeO2 nanocomposites synthesized by green method. Int J Hydrogen Energy 2017 May 25;42(21):14608–20.
[175] Gholami T, Salavati-Niasari M. Green facile thermal decomposition synthesis, characterization and electrochemical hydrogen storage characteristics of ZnAl2O4 nanostructure. Int J Hydrogen Energy 2017 Jul 6;42(27):17167–77.
[176] Masjedi-Arani M, Salavati-Niasari M. Novel synthesis of Zn2GeO4/graphene nanocomposite for enhanced electrochemical hydrogen storage performance. Int J Hydrogen Energy 2017 Jul 6;42(27):17184–91.
[177] Sangsefidi FS, Salavati-Niasari M. Thermal decomposition synthesis, characterization and electrochemical hydrogen storage characteristics of Co3O4–CeO2 porous nanocomposite. Int J Hydrogen Energy 2017 Aug 3;42(31):20071–81.
[178] Sangsefidi FS, Salavati-Niasari M, Varshoy S, Shabani-Nooshabadi M. Investigation of Mn2O3 as impurity on the electrochemical hydrogen storage performance of MnO2CeO2 nanocomposites. Int J Hydrogen Energy 2017 Nov 23;42(47):28473–84.
[179] Salehabadi A, Salavati-Niasari M, Ghiyasiyan-Arani M. Self-assembly of hydrogen storage materials based multi-walled carbon nanotubes (MWCNTs) and Dy3Fe5O12 (DFO) nanoparticles. J Alloy Comp 2018 May 15;745:789–97.
[180] Salehabadi A, Salavati-Niasari M, Gholami T. Green and facial combustion synthesis of Sr3Al2O6 nanostructures; a potential electrochemical hydrogen storage material. J Clean Prod 2018 Jan 10;171:1–9.
[181] Gholami T, Salavati-Niasari M, Salehabadi A, Amiri M, Shabani-Nooshabadi M, Rezaie M. Electrochemical hydrogen storage properties of NiAl2O4/NiO nanostructures using TiO2, SiO2 and graphene by auto-combustion method using green tea extract. Renew Energy 2018 Jan 1;115:199–207.
[182] Masjedi-Arani M, Salavati-Niasari M. Facile precipitation synthesis and electrochemical evaluation of Zn2SnO4 nanostructure as a hydrogen storage material. Int J Hydrogen Energy 2017 Apr 27;42(17):12420–9.
[183] Escobar DP, Depover T, Duprez L, Verbeken K, Verhaege M. Combined thermal desorption spectroscopy, differential scanning calorimetry, scanning electron microscopy and X-ray diffraction study of hydrogen trapping in cold deformed TRIP steel. Acta Mater 2012 Apr 1;60(6–7):2593–605.

[184] Depover T, Monbaliu O, Wallaert E, Verbeken K. Effect of Ti, Mo and based precipitates on the hydrogen trapping and embrittlement of FeeCeX Q&T alloys. Int J Hydrogen Energy 2015;40(16977):16984.
[185] Depover T, Verbeken K. Hydrogen trapping and hydrogen induced mechanical degradation in lab cast Fe-C-Cr alloys. Mater Sci Eng A 2016 Jul 4;669:134–49.
[186] Depover T, Verbeken K. Thermal desorption spectroscopy study of the hydrogen trapping ability of W based precipitates in a Q&T matrix. Int J Hydrogen Energy 2018 Mar 15;43(11):5760–9.
[187] Depover T, Verbeken K. The effect of TiC on the hydrogen induced ductility loss and trapping behavior of Fe-C-Ti alloys. Corros Sci 2016 Nov 1;112:308–26.
[188] Loidl M, Kolk O. Hydrogen Embrittlement in HSSs Limits Use in Lightweight Body in White Design-High strength steels (HSSs) can fail due to hydrogen embrittlement under certain circumstances, which hinders their use in the body in white design. Adv Mater Process 2011;169(3):22.
[189] Loidl M, Kolk O, Veith S, Göbel T. Characterization of hydrogen embrittlement in automotive advanced high strength steels. Mater Werkst 2011 Dec;42(12):1105–10.
[190] Loidl M. Development of a test methodology for characterizing high-strength body steels with respect to the risk of hydrogen-induced cracking. 2014.
[191] Esteban RM, Schütte K, Marquardt D, Barthel J, Beckert F, Mülhaupt R, Janiak C. Synthesis of ruthenium@ graphene nanomaterials in propylene carbonate as re-useable catalysts for the solvent-free hydrogenation of benzene. Nano-Structures & Nano-Objects 2015 Aug 1;2:28–34.
[192] de Yuso Alicia M, Oumellal Y, Zlotea C, Vidal L, Camelia MG. In-situ Pd–Pt nanoalloys growth in confined carbon spaces and their interactions with hydrogen. Nano-Structures & Nano-Objects 2017 Feb 1;9:1–2.
[193] Oumellal Y, Ghimbeu CM, de Yuso AM, Zlotea C. Hydrogen absorption properties of carbon supported Pd–Ni nanoalloys. Int J Hydrogen Energy 2017 Jan 12;42(2):1004–11.
[194] Esteban RM, Schütte K, Brandt P, Marquardt D, Meyer H, Beckert F, Mülhaupt R, Kölling H, Janiak C. Iridium@ graphene composite nanomaterials synthesized in ionic liquid as re-useable catalysts for solvent-free hydrogenation of benzene and cyclohexene. Nano-Structures & Nano-Objects 2015 Aug 1;2:11–8.
[195] Zlotea C, Oumellal Y, Berrú JJ, Aguey-Zinsou KF. On the feasibility of the bottom-up synthesis of Mg2CoH5 nanoparticles supported on a porous carbon and their hydrogen desorption behaviour. Nano-Structures & Nano-Objects 2018 Oct 1;16:144–50.
[196] Oumellal Y, Joubert JM, Ghimbeu CM, Le Meins JM, Bourgon J, Zlotea C. Synthesis and stability of Pd–Rh nanoalloys with fully tunable particle size and composition. Nano-Structures & Nano-Objects 2016 Jul 1;7:92–100.
[197] Yang F, Tang J, Shao B, Gao S, Liu X. Ni-bearing nanoporous alumina loaded ultralow-concentrated Pd as robust dual catalyst toward hydrogenation and oxidation reactions. Nano-Structures & Nano-Objects 2019 Apr 1;18. 100287.
[198] Betsy KJ, Lazar A, Vinod CP. Highly selective aqueous phase hydrogenation of phenols over nanostructured RuO2 on MCM-41 catalysts. Nano-Structures & Nano-Objects 2018 Feb 1;13:36–43.